

CT14 Global Analysis and CT14QED

Carl Schmidt
Michigan State University

On behalf of the CTEQ-TEA group

October 19, 2015
INT-15-3 Program

CTEQ-TEA group

- CTEQ – Tung et al. (TEA)

In memory of **Prof. Wu-Ki Tung**,
who established CTEQ Collaboration in early 90's

- Current members of CTEQ-TEA group:

Sayipjamal Dulat (Xinjiang U.)

Tie-Jiun Hou, Pavel Nadolsky (Southern Methodist U.)

Jun Gao (Argonne Nat. Lab.)

Marco Guzzi (U. of Manchester)

Joey Huston, Jon Pumplin, Dan Stump, CS, C.-P. Yuan (Michigan State U.)

Outline

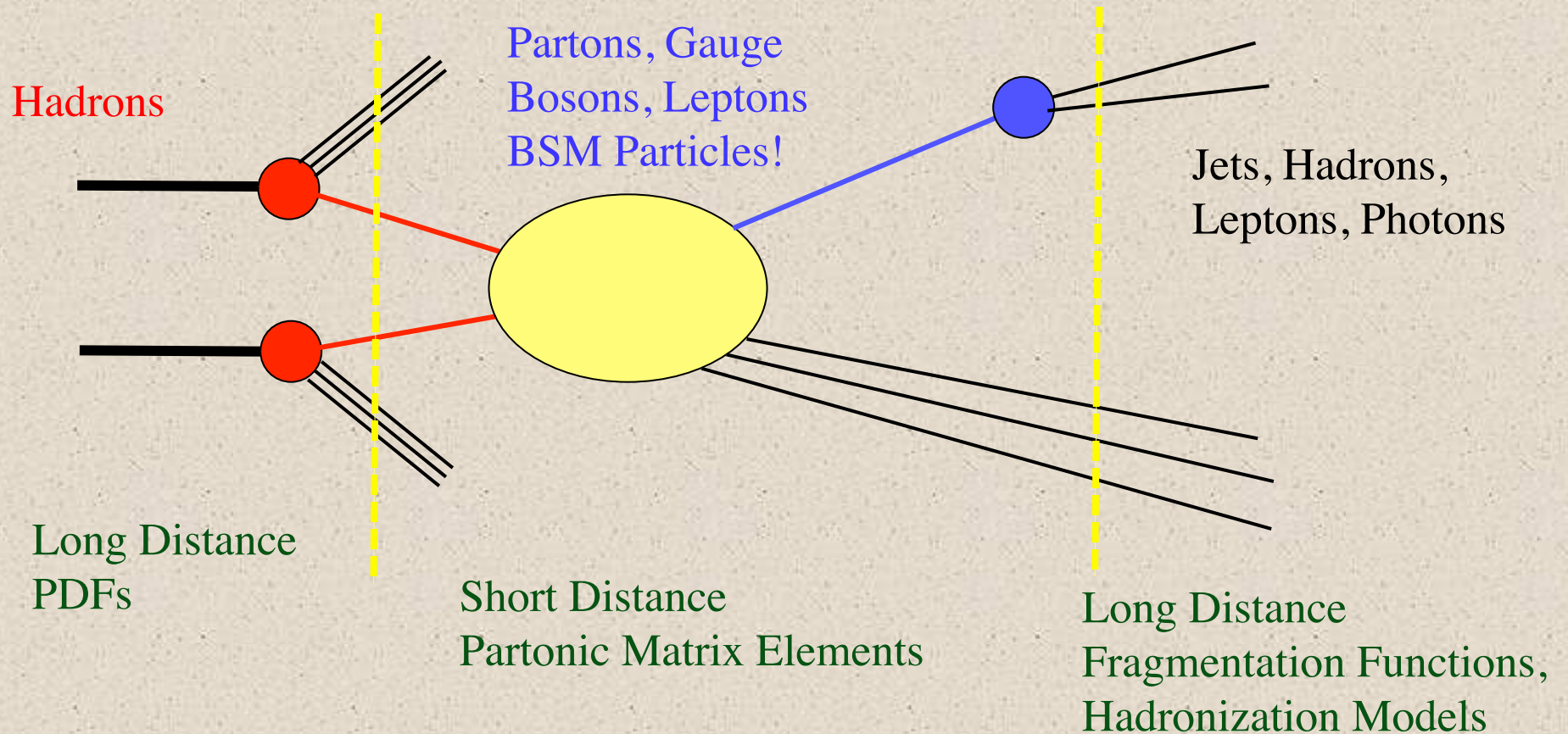
1) **CT14 Global Analysis of Quantum Chromodynamics**

Dulat et al, ArXiv:1506.07433[hep-ph]

2) **CT14QED PDFs from Isolated Photon Production in DIS**

CS, J. Pumplin, D. Stump, C.-P, Yuan, arXiv:1509.02905[hep-ph]

Hadron Collider Physics



$$\sigma(p_1 p_2 \rightarrow H + X) = \sum_{a,b} \int dx_1 \int dx_2 f_{a/p_1}(x_1, \mu) f_{b/p_2}(x_2, \mu) \hat{\sigma}^{ab}(x_1 x_2 s, \mu) + O\left(\frac{\Lambda^2}{Q^2}\right)$$

Parton Density Functions

- PDFs difficult to calculate theoretically from first principles (although work in that direction being done)
- Therefore, extract from experimental data
- PDFs are universal
 - DIS in lepton-hadron colliders
 - Drell-Yan, Vector Boson Production in hadron-hadron colliders
 - Jet production in hadron-hadron colliders
- Global analysis to extract PDFs from multiple data inputs
 - Different data probes unique combinations of partonic PDFs

Importance of PDFs

- Higher order (NLO, NNLO, etc) in QCD requires comparable precision
 - $gg \Rightarrow$ Higgs at N³LO!, errors from PDFs comparable or larger than renormalization/factorization uncertainties
- Are discrepancies from SM signs of new physics?
 - Counting experiments (single top, SUSY, ...) require well-understood signal and background \Rightarrow PDFs
 - Precision Higgs and top measurements
 - Gauge Boson, Jet cross section predictions
 - influenced by PDF assumptions?
- EW corrections \Rightarrow photon PDFs, may have important contributions (WW at high \sqrt{s} ?)

CT14 Global Analysis - Data

Minimize $\chi^2 = \sum_{\alpha=1}^N \chi_{\alpha}^2$ with $\chi_{\alpha}^2 = \sum_{i=1}^{N_{\alpha}} \left(\frac{\text{data}_i - \text{theory}_i}{\text{error}_i} \right)^2$

$N = 33$ Experiments, $N \cdot N_{\alpha} = 2947$ data points
Careful treatment of Correlated systematic errors

ID#	Experimental data set	$N_{pt,n}$	χ_n^2	$\chi_n^2/N_{pt,n}$	S_n
101	BCDMS F_2^p [24]	337	384	1.14	1.74
102	BCDMS F_2^d [25]	250	294	1.18	1.89
104	NMC F_2^d/F_2^p [26]	123	133	1.08	0.68
106	NMC σ_{red}^p [26]	201	372	1.85	6.89
108	CDHSW F_2^p [27]	85	72	0.85	-0.99
109	CDHSW F_3^p [27]	96	80	0.83	-1.18
110	CCFR F_2^p [28]	69	70	1.02	0.15
111	CCFR xF_3^p [29]	86	31	0.36	-5.73
124	NuTeV $\nu\mu\mu$ SIDIS [30]	38	24	0.62	-1.83
125	NuTeV $\bar{\nu}\mu\mu$ SIDIS [30]	33	39	1.18	0.78
126	CCFR $\nu\mu\mu$ SIDIS [31]	40	29	0.72	-1.32
127	CCFR $\bar{\nu}\mu\mu$ SIDIS [31]	38	20	0.53	-2.46
145	H1 σ_r^b [32]	10	6.8	0.68	-0.67
147	Combined HERA charm production [33]	47	59	1.26	1.22
159	HERA1 Combined NC and CC DIS [34]	579	591	1.02	0.37
169	H1 F_L [35]	9	17	1.92	1.7

ID#	Experimental data set	$N_{pt,n}$	χ_n^2	$\chi_n^2/N_{pt,n}$	S_n
201	E605 Drell-Yan process [37]	119	116	0.98	-0.15
203	E866 Drell-Yan process, $\sigma_{pd}/(2\sigma_{pp})$ [38]	15	13	0.87	-0.25
204	E866 Drell-Yan process, $Q^3 d^2\sigma_{pp}/(dQdx_F)$ [39]	184	252	1.37	3.19
225	CDF Run-1 electron A_{ch} , $p_{T\ell} > 25$ GeV [40]	11	8.9	0.81	-0.32
227	CDF Run-2 electron A_{ch} , $p_{T\ell} > 25$ GeV [41]	11	14	1.24	0.67
234	DØ Run-2 muon A_{ch} , $p_{T\ell} > 20$ GeV [42]	9	8.3	0.92	-0.02
240	LHCb 7 TeV 35 pb ⁻¹ W/Z $d\sigma/dy_{\ell}$ [43]	14	9.9	0.71	-0.73
241	LHCb 7 TeV 35 pb ⁻¹ A_{ch} , $p_{T\ell} > 20$ GeV [43]	5	5.3	1.06	0.30
260	DØ Run-2 Z rapidity [44]	28	17	0.59	-1.71
261	CDF Run-2 Z rapidity [45]	29	48	1.64	2.13
266	CMS 7 TeV 4.7 fb ⁻¹ , muon A_{ch} , $p_{T\ell} > 35$ GeV [46]	11	12.1	1.10	0.37
267	CMS 7 TeV 840 pb ⁻¹ , electron A_{ch} , $p_{T\ell} > 35$ GeV [47]	11	10.1	0.92	-0.06
268	ATLAS 7 TeV 35 pb ⁻¹ W/Z cross sec., A_{ch} [48]	41	51	1.25	1.11
281	DØ Run-2 9.7 fb ⁻¹ electron A_{ch} , $p_{T\ell} > 25$ GeV [14]	13	35	2.67	3.11
504	CDF Run-2 inclusive jet production [49]	72	105	1.45	2.45
514	DØ Run-2 inclusive jet production [50]	110	120	1.09	0.67
535	ATLAS 7 TeV 35 pb ⁻¹ incl. jet production [51]	90	50	0.55	-3.59
538	CMS 7 TeV 5 fb ⁻¹ incl. jet production [52]	133	177	1.33	2.51

CT14 Global Analysis - Data

Minimize $\chi^2 = \sum_{\alpha=1}^N \chi_{\alpha}^2$ with $\chi_{\alpha}^2 = \sum_{i=1}^{N_{\alpha}} \left(\frac{\text{data}_i - \text{theory}_i}{\text{error}_i} \right)^2$

$N = 33$ Experiments, $N \cdot N_{\alpha} = 2947$ data points
Careful treatment of Correlated systematic errors

ID#	Experimental data set	$N_{pt,n}$	χ_n^2	$\chi_n^2/N_{pt,n}$	S_n
101	BCDMS F_2^p [24]	337	384	1.14	1.74
102	BCDMS F_2^d [25]	250	294	1.18	1.89
104	NMC F_2^d/F_2^p [26]	123	133	1.08	0.68
106	NMC σ_{red}^p [26]	201	372	1.85	6.89
108	CDHSW F_2^p [27]	85	72	0.85	-0.99
109	CDHS F_2^p [28]	5	80	0.83	-1.18
110	CCFR F_2^p [29]	9	70	1.02	0.15
111	CCFR xF_3^p [29]	86	31	0.36	-5.73
124	NuTeV $\nu\mu\mu$ SIDIS [30]	38	24	0.62	-1.83
125	NuTeV $\bar{\nu}\mu\mu$ SIDIS [30]	33	39	1.18	0.78
126	CCFR $\nu\mu\mu$ SIDIS [31]	40	29	0.72	-1.32
127	CCFR $\bar{\nu}\mu\mu$ SIDIS [31]	38	20	0.53	-2.46
145	H1 F_2^p [32]	10	6.8	0.68	-0.67
147	Combined HERA charm production [33]	47	1.26	1.22	
159	HERA-1 Combined NC and CC DIS [34]	579	591	1.02	0.37
169	H1 F_L [35]	9	17	1.92	1.7

New for CT14

ID#	Experimental data set	$N_{pt,n}$	χ_n^2	$\chi_n^2/N_{pt,n}$	S_n
201	E605 Drell-Yan process [37]	119	116	0.98	-0.15
203	E866 Drell-Yan process, $\sigma_{pd}/(2\sigma_{pp})$ [38]	15	13	0.87	-0.25
204	E866 Drell-Yan process, $Q^3 d^2\sigma_{pp}/(dQdx_F)$ [39]	184	252	1.37	3.19
225	CDF Run-1 electron A_{ch} , $p_{T\ell} > 25$ GeV [40]	11	8.9	0.81	-0.32
227	CDF Run-2 electron A_{ch} , $p_{T\ell} > 25$ GeV [41]	11	14	1.24	0.67
234	DØ Run-2 muon A_{ch} , $p_{T\ell} > 20$ GeV [42]	9	8.3	0.92	-0.02
240	LHCb 7 TeV 35 pb ⁻¹ W/Z $d\sigma/dy_{\ell}$ [43]	14	9.9	0.71	-0.73
241	LHCb 7 TeV 35 pb ⁻¹ A_{ch} , $p_{T\ell} > 20$ GeV [43]	5	5.3	1.06	0.30
260	DØ Run-2 Z rapidity [44]	28	17	0.59	-1.71
261	CDF Run-2 Z rapidity [45]	29	48	1.64	2.13
266	CMS 7 TeV 4.7 fb ⁻¹ , muon A_{ch} , $p_{T\ell} > 35$ GeV [46]	1	12.1	1.10	0.37
267	CMS 7 TeV 840 pb ⁻¹ , electron A_{ch} , $p_{T\ell} > 35$ GeV [47]	1	10.1	0.92	-0.06
268	ATLAS 7 TeV 35 pb ⁻¹ W/Z cross sec., A_{ch} [48]	1	51	1.25	1.11
281	DØ Run-2 9.7 fb ⁻¹ electron A_{ch} , $p_{T\ell} > 25$ GeV [14]	3	35	2.67	3.11
504	CDF Run-2 inclusive jet production [49]	72	105	1.45	2.45
514	DØ Run-2 inclusive jet production [50]	110	120	1.09	0.67
535	ATLAS 7 TeV 35 pb ⁻¹ incl. jet production [51]	90	50	0.55	-3.59
538	CMS 7 TeV 5 fb ⁻¹ incl. jet production [52]	133	177	1.33	2.51

CT14 Global Analysis - Theory

Theory Input:

- Parametrize PDFs at $Q_0=1.295$ GeV

$$xf_a(x, Q_0) = x^{a_1} (1-x)^{a_2} P_a(x)$$

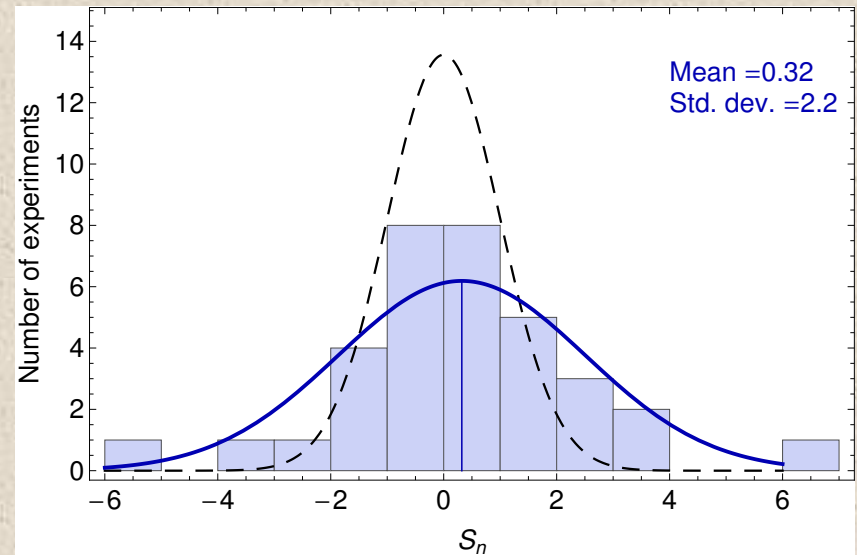
- $P_a(x)$ are Bernstein Polynomials
 - Less correlations between parameters, better control at $x \rightarrow 0, 1$
- Increase number of parameters in CT14 for more flexibility
 - 28 parameters for CT14 vs 25 for CT10
 - Most visible in gluon, d/u at large x, both d/u, dbar/ubar at small x and s quarks (assume $s=\bar{s}$)
- Use S-ACOT- χ for heavy quarks ($m_c=1.3$ GeV, $m_b=4.75$ GeV pole mass)
- For NNLO PDFs use NNLO calculations for all except jet production and DIS CC (use NLO for NNLO PDFs)
- Only use data with $Q^2 > 4$ GeV² and $W^2 > 12.6$ GeV² to minimize nonperturbative effects

CT14 PDF Error Estimation

First consider consistency of data:

Map χ^2 distribution $(\chi_n^2, N_n) \rightarrow S_n$ “Effective Gaussian Variable”
for each experiment

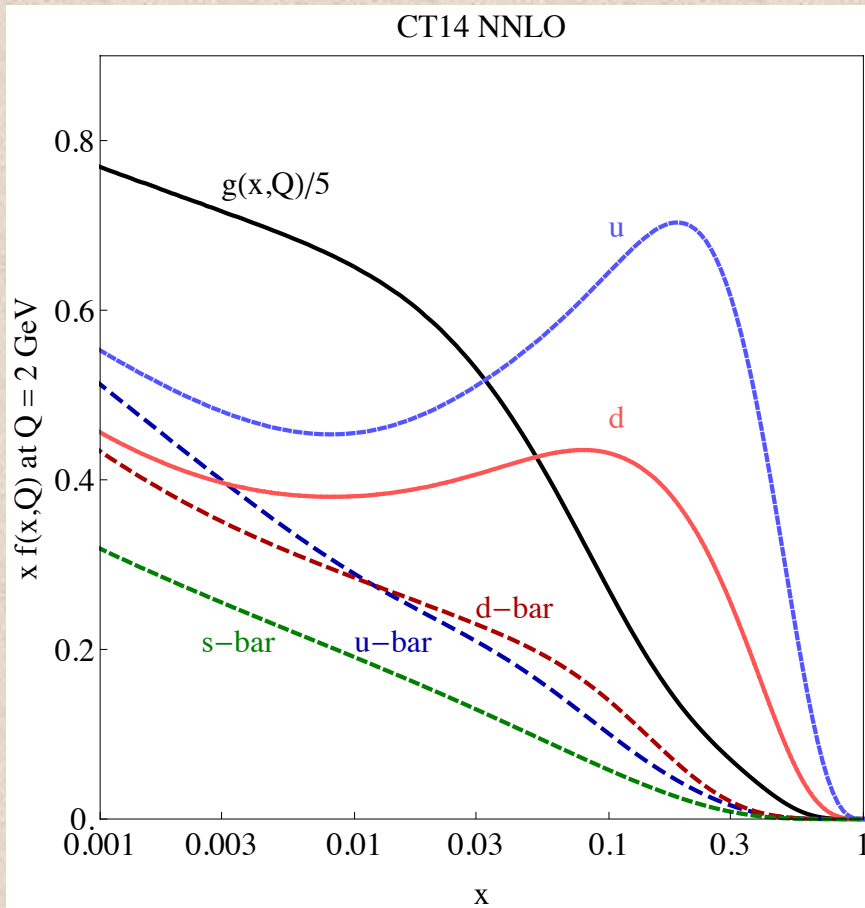
- $-1 < S_n < 1$ is good fit
- $S_n > 2$ is bad fit
- $S_n < -2$ is anomalously good fit
- Ideal distribution would have Std. dev.=1



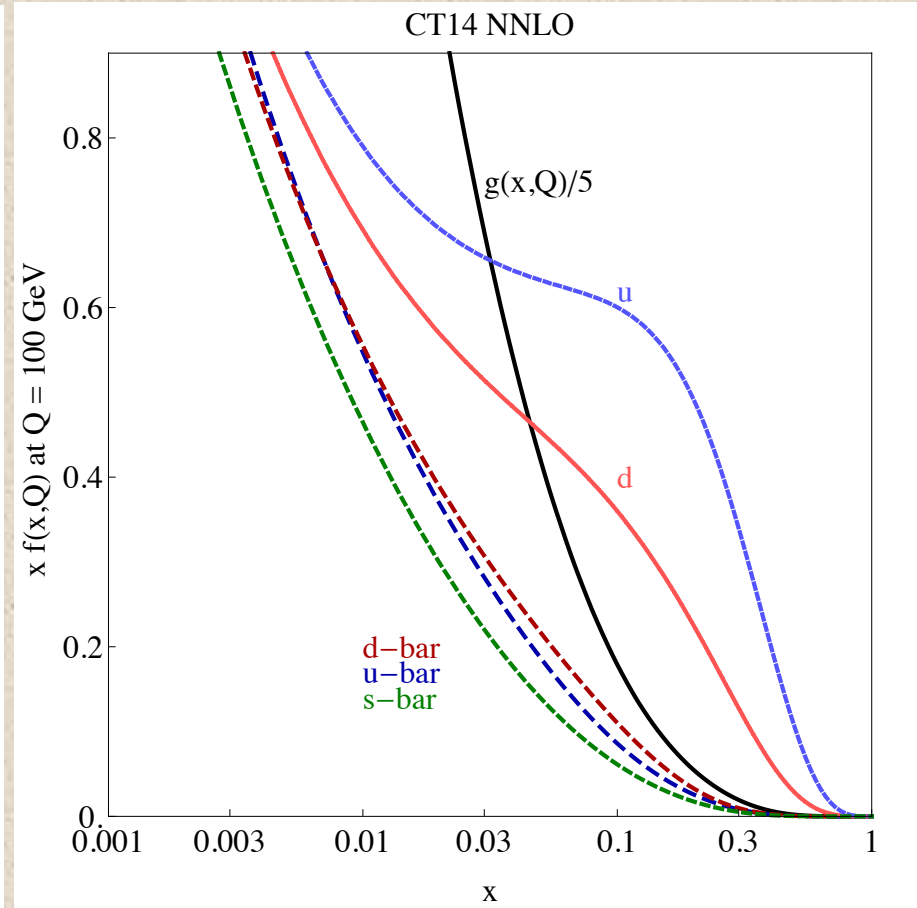
Hessian Method

- 56 Eigenvector sets, to estimate errors for observables
- 90% CL tolerance $\Delta\chi^2 < T^2=100$ (68% CL= $\Rightarrow T/1.645$)
- Also require no particular experiment is fit too badly, using S_n . (Tier 2 penalty)
- Assumes quadratic dependence of χ^2 and linear dependence of observables on PDF parameters around minimum
- Lagrange Multiplier Method used to confirm Hessian results

The CT14 PDFs

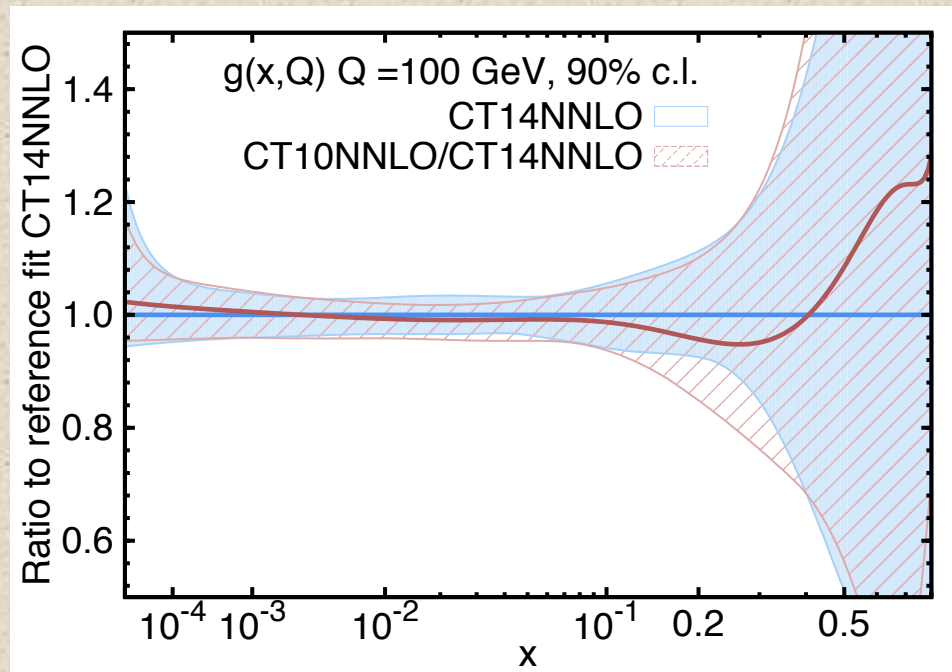


$Q = 2 \text{ GeV}$



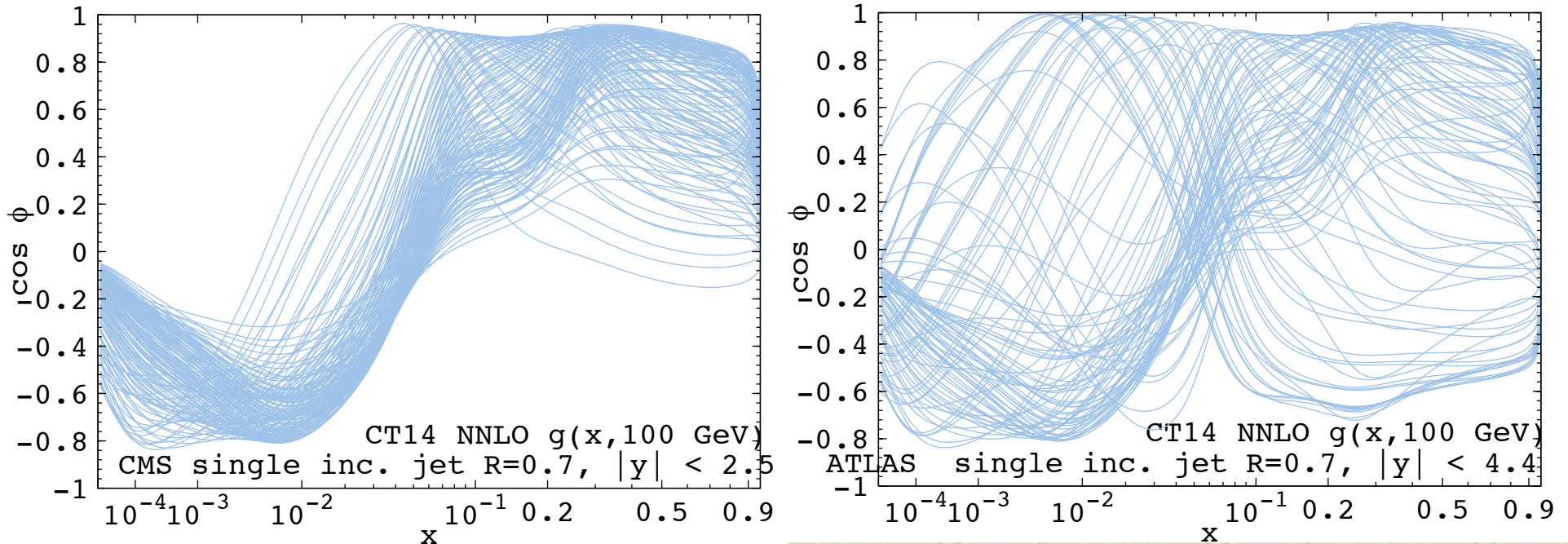
$Q = 100 \text{ GeV}$

CT14 gluon PDF



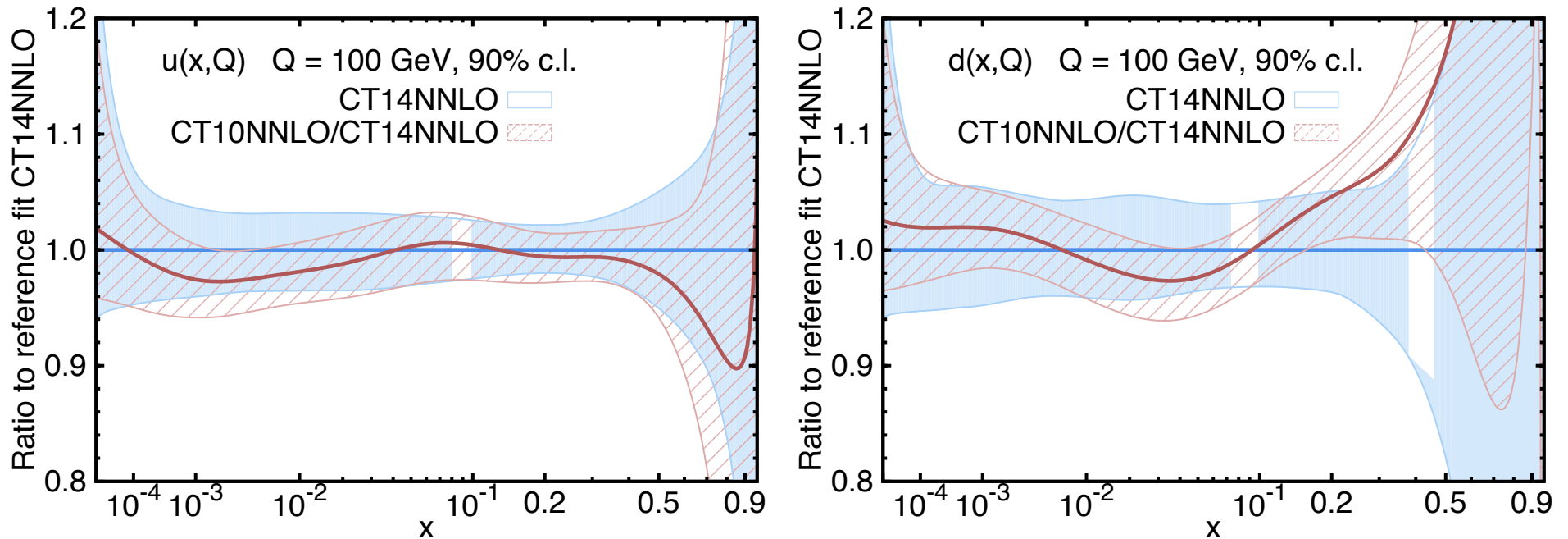
- Gluon has increased 1-2% over CT10 for most of the range
- But still within CT10 errors
- Due partially to CMS data

CT14 gluon PDF



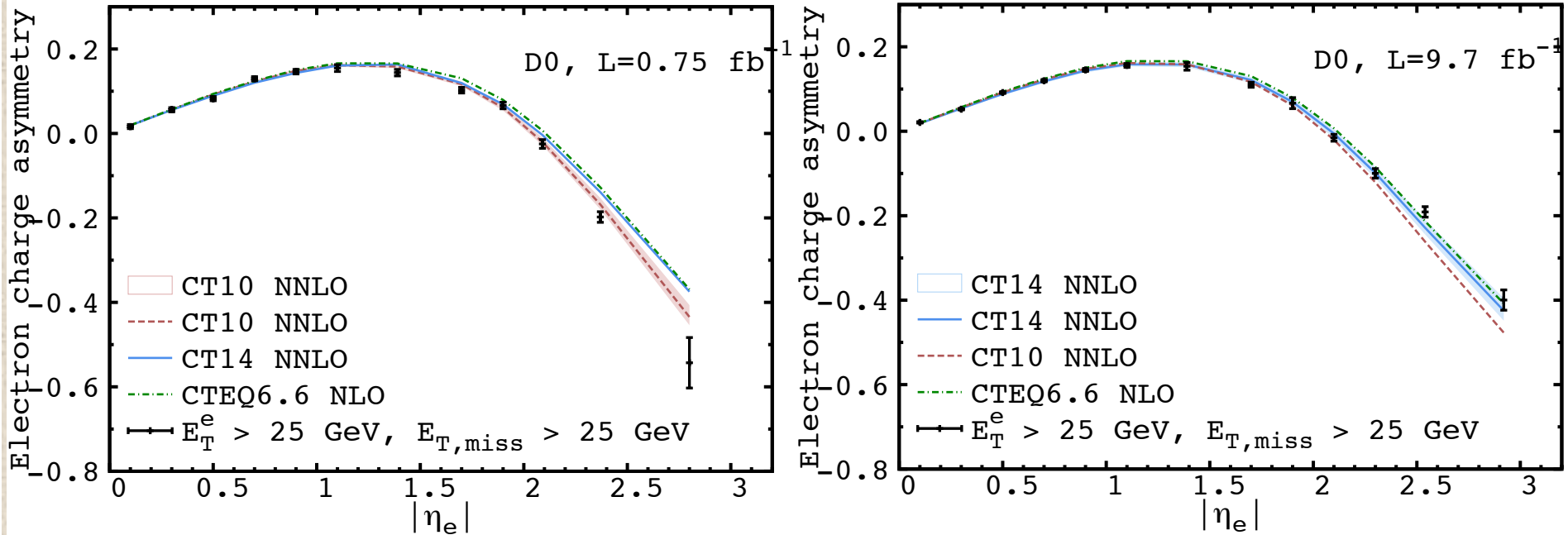
- Correlation Cosine between Data points and $f_g(x)$
- 1=Strong correlation, -1=Strong Anticorrelation
- CMS and ATLAS correlated over larger range of x than CDF/D0
- (Especially ATLAS, because of large rapidity range)
- However, ATLAS errors still large

CT14 valence quark PDFs



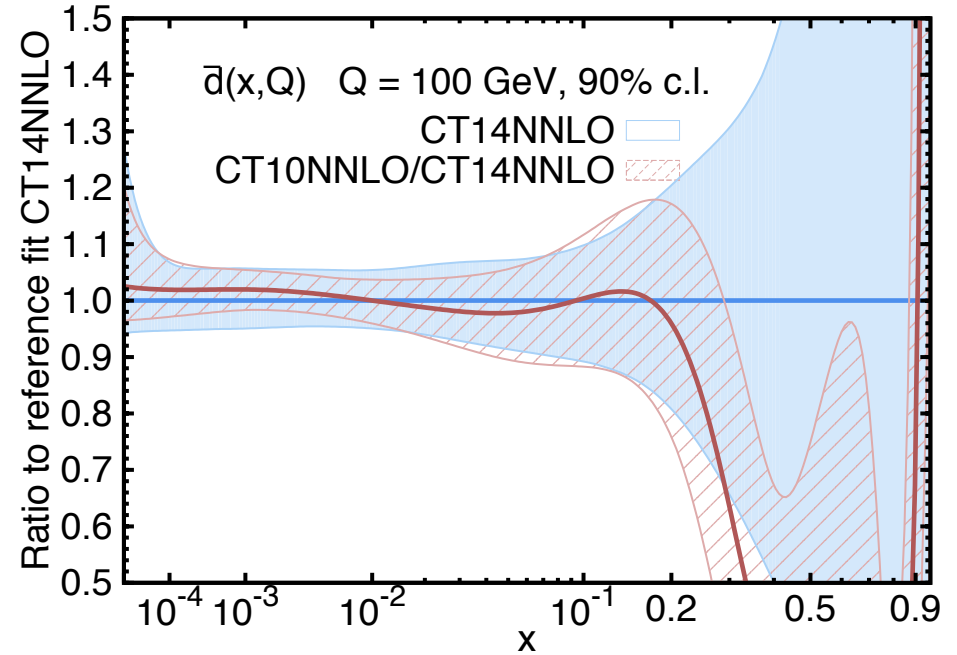
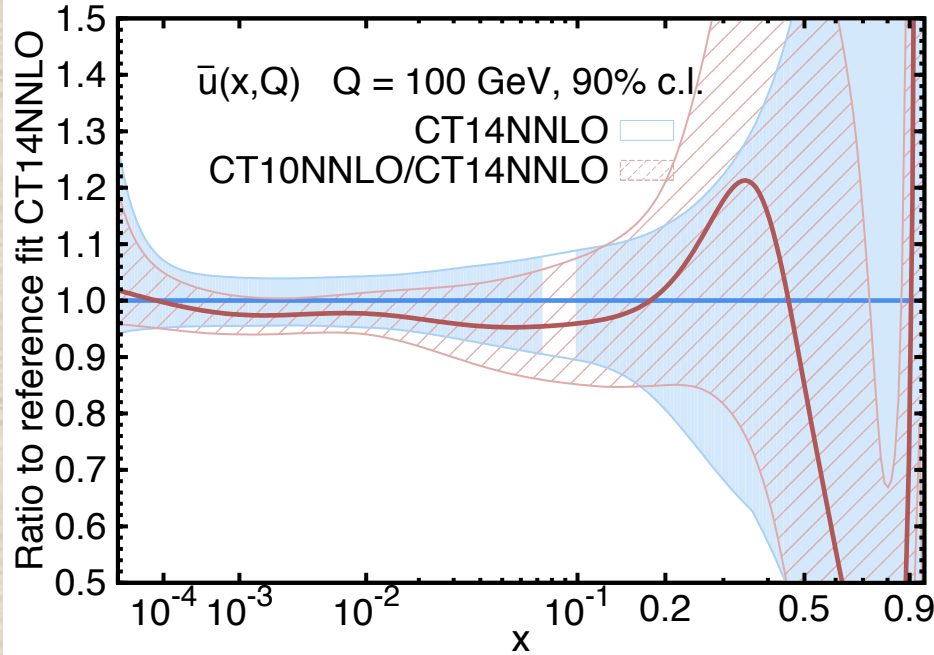
- Increase in u and decrease in d at small $x \sim 10^{-3}$ due to increased flexibility of parametrization
- Increase in d at $x \sim 0.05$ due to ATLAS/CMS/LHCb W/Z data
- Increase in u, decrease in d at large x, due to updated D0 charge asymmetry (also parametrization)

CT14 valence quark PDFs



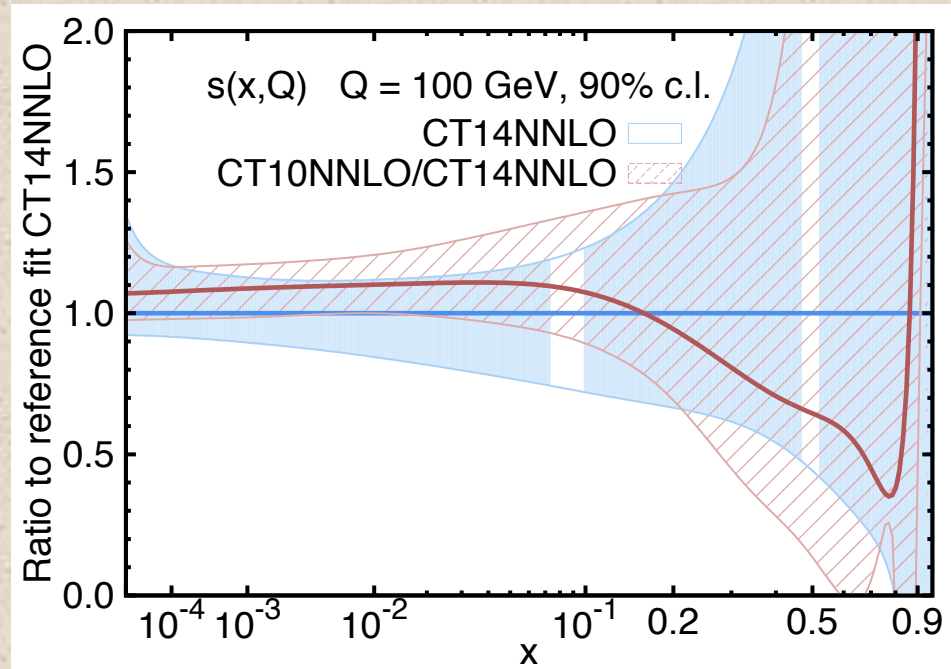
- Replacing old ($L=0.75 \text{ fb}^{-1}$) D0 data with new ($L=9.7 \text{ fb}^{-1}$) moves CT14 closer to earlier CTEQ6.6 than CT10.
- Reduces d/u for $x > 0.1$

CT14 sea quark PDFs



- Change in behavior of \bar{d}/\bar{u} at $x < 10^{-3}$ and $x > 0.2$ due to parametrization, but data constraints are weak in that range
- In middle range of x , both \bar{u} and \bar{d} have increased over CT10

CT14 strange quark PDF



- Assumed $s=\bar{s}$
- In region constrained by data, s has decreased sizably, but still within uncertainty limits of CT10
- Due to multiple factors
- LHC measurements of $W+c$ may provide information on $s-\bar{s}$

CT14 strange quark PDF

- Conflicting results from experiments:

- **ATLAS** $r^s = \frac{\bar{s}(x, Q)}{\bar{d}(x, Q)} = 0.96_{-0.30}^{+0.26}$ at $x = 0.023$, $Q = 1.4$ GeV

$$r_{\text{CT14NNLO}}^s = 0.53 \pm 0.20$$

$$r_{\text{CT10NNLO}}^s = 0.76 \pm 0.17$$

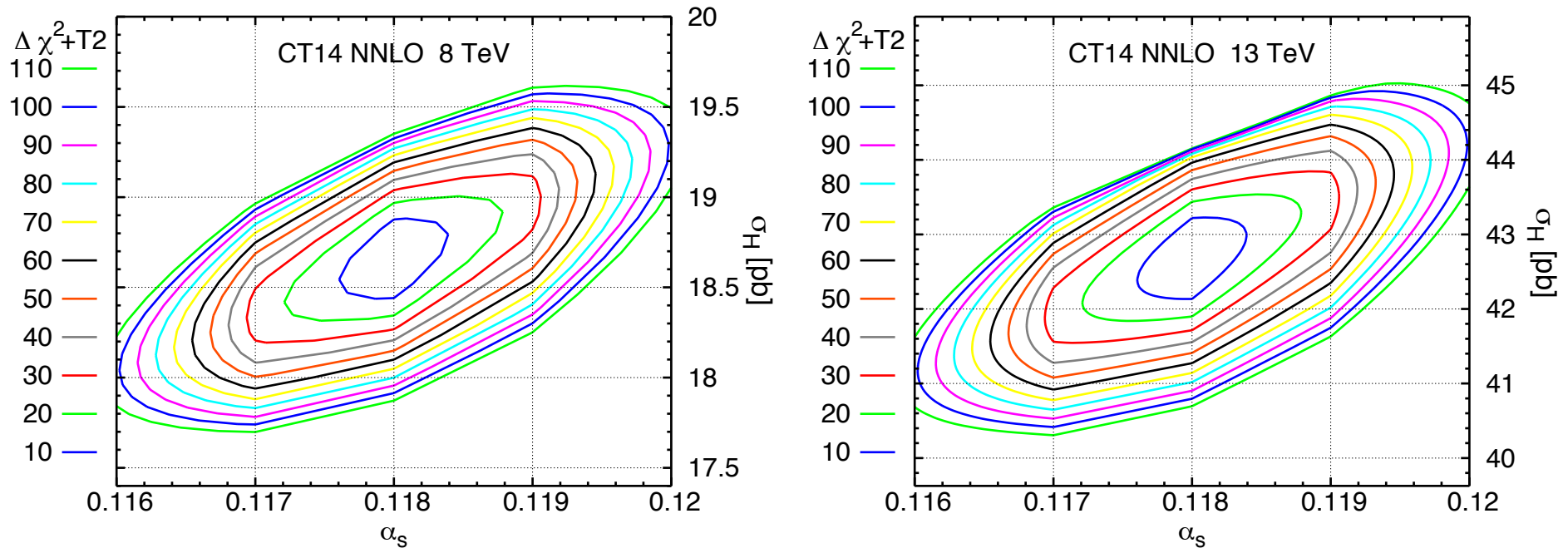
- **CMS** $K^s = \frac{\int_0^1 x [s(x, Q) + \bar{s}(x, Q)] dx}{\int_0^1 x [\bar{u}(x, Q) + \bar{d}(x, Q)] dx} = 0.52_{-0.15}^{+0.18}$ at $Q^2 = 20$ GeV²

- **NOMAD** $K^s = 0.591 \pm 0.019$

$$K_{\text{CT14NNLO}}^s = 0.62 \pm 0.14$$

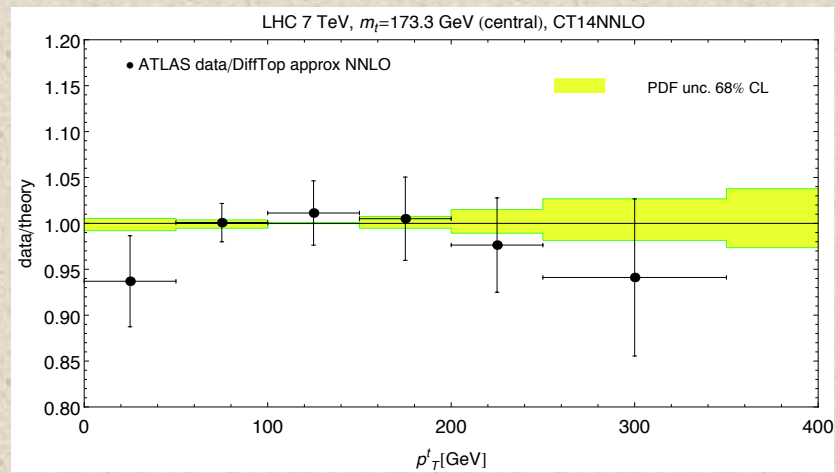
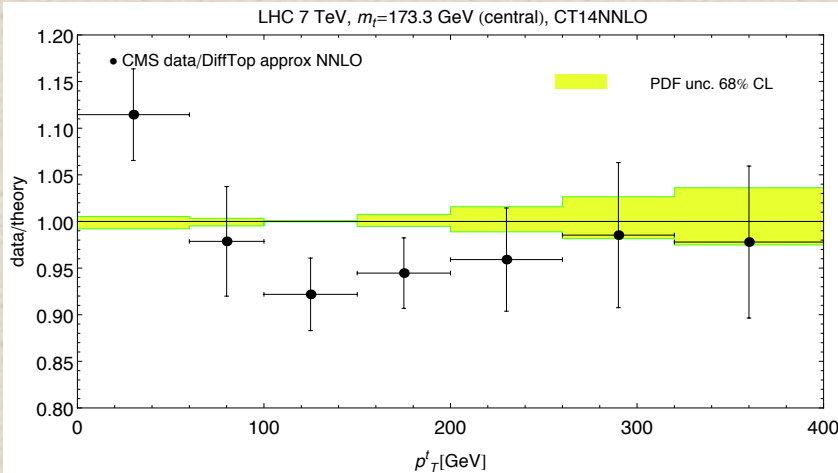
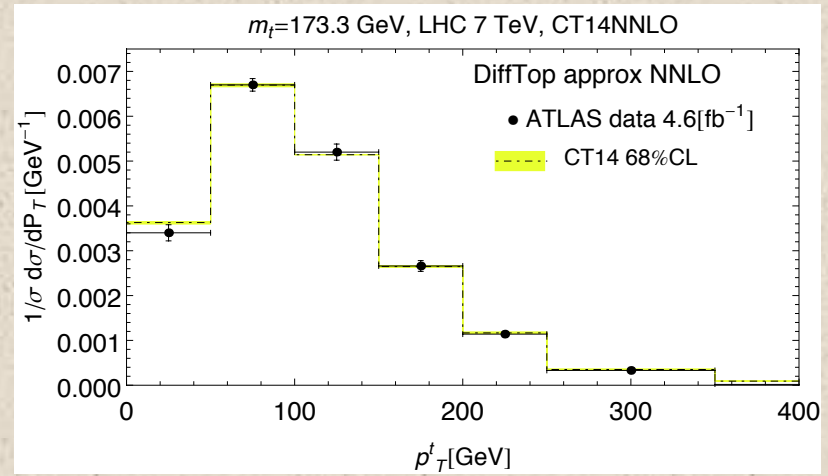
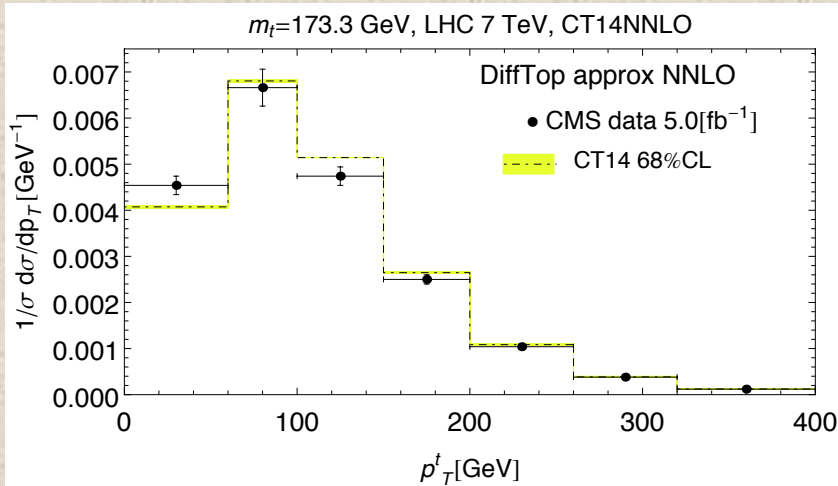
$$K_{\text{CT10NNLO}}^s = 0.73 \pm 0.11$$

PDF uncertainties on $gg \rightarrow H$



- Error ellipse computed using with iHixs, using Lagrange Multiplier method
- Strong correlation between α_s and cross section
- Central value prediction agrees perfectly with MMHT2014 and NNPDF3.0

PDFs and $t\bar{t}$ production



- Computed with DiffTop (Guzzi, Lipka, Moch JHEP 2014)
- CT14 PDF errors are smaller than experimental errors

Other PDF Sets

- CT14NLO, including Hessian error sets
- CT14LO, with 1-loop or 2-loop running of α_s
- Series of (N)NLO with $\alpha_s(M_Z)=0.111 - 0.123$
- Sets with Heavy Quark schemes with up to 3, 4, and 6 active flavors
- Sets with nonperturbative charm
- Sets which include QED evolution at order α

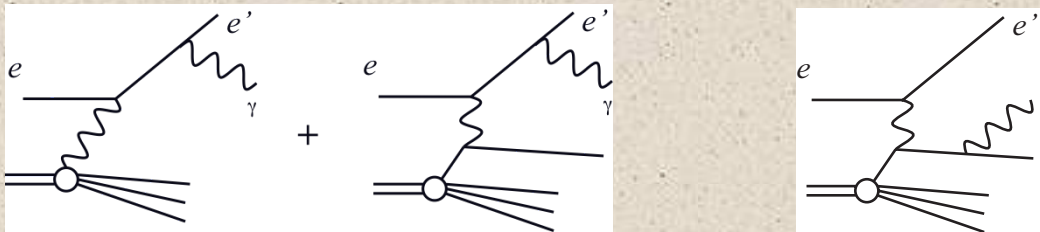
CT14QED PDFs

1) Previous studies

- a) **MRST** Martin et al., EPJC 39 (2005) 155
 - Radiation off “primordial current quark” distributions
- b) **NNPDF** Ball et al., Nuc. Phys. B 877 (2013) 290
 - parametrized fit, predominantly constrained by W, Z, γ^* Drell-Yan

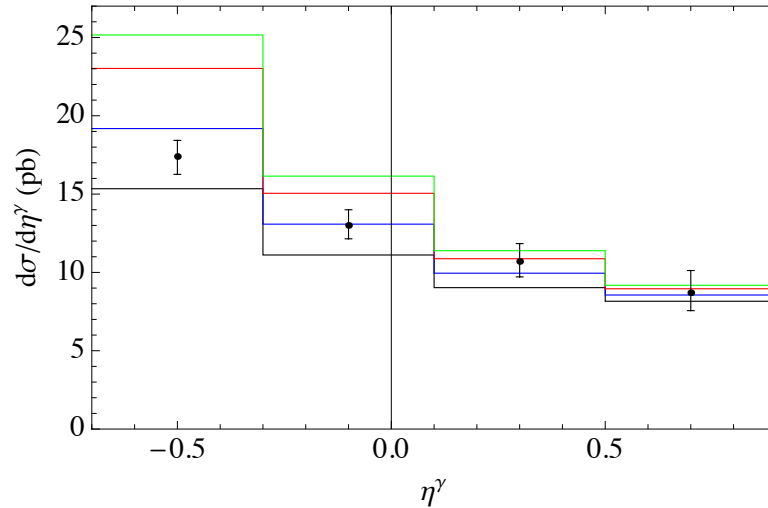
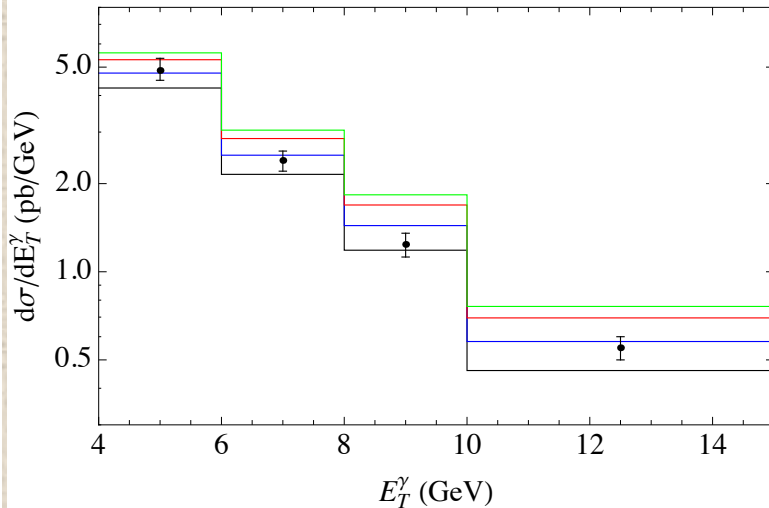
2) First CT QED PDF set

- Evolve α at LO and α_s at NLO
- Photon PDF is one-parameter generalization of radiative ansatz off CT14NLO, specified by initial photon momentum fraction p_0^γ at $Q_0=1.295$ GeV
- Constrained by ZEUS DIS + isolated photon data $ep \rightarrow e\gamma + X$
- Required new calculation, consistently combining photon-initiated contributions and quark initiated contributions



Distributions

1) Photon Variables E_T^γ and η^γ



$p_0^\gamma = p_0^\gamma$ (cm)
 $= 0.29\%$
 $p_0^\gamma = 0.2\%$
 $p_0^\gamma = 0.1\%$
 $p_0^\gamma = 0.0\%$

(Smooth Isolation, $\mu_F = 0.5E_T^\gamma$)

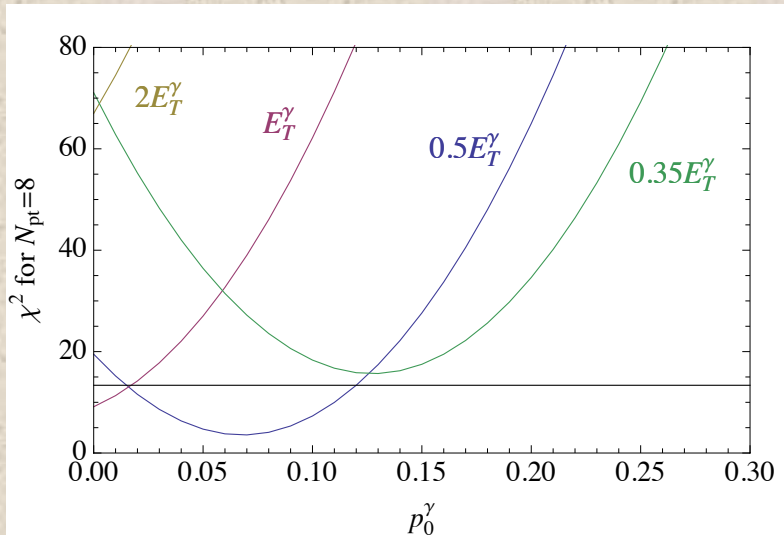
- Theoretical uncertainties due to factorization scale, and isolation prescription
- We used two isolation models:

- Frixione smooth isolation $E_{q'} < \frac{1}{9} E_\gamma \left(\frac{1 - \cos r}{1 - \cos R} \right)$ for $r = \sqrt{\Delta\eta_{q'\gamma}^2 + \Delta\varphi_{q'\gamma}^2} < R = 1$

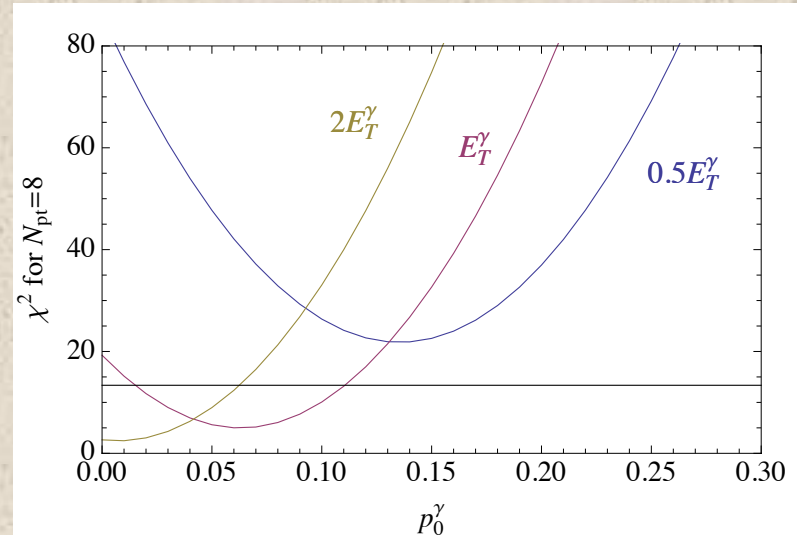
- Sharp isolation with photon fragmentation function

$$E_{q'} < \frac{1}{9} E_\gamma \quad \text{for } r < R = 1 \quad (\text{Use Aleph LO fragmentation})$$

Limits on Photon PDF



Smooth Isolation



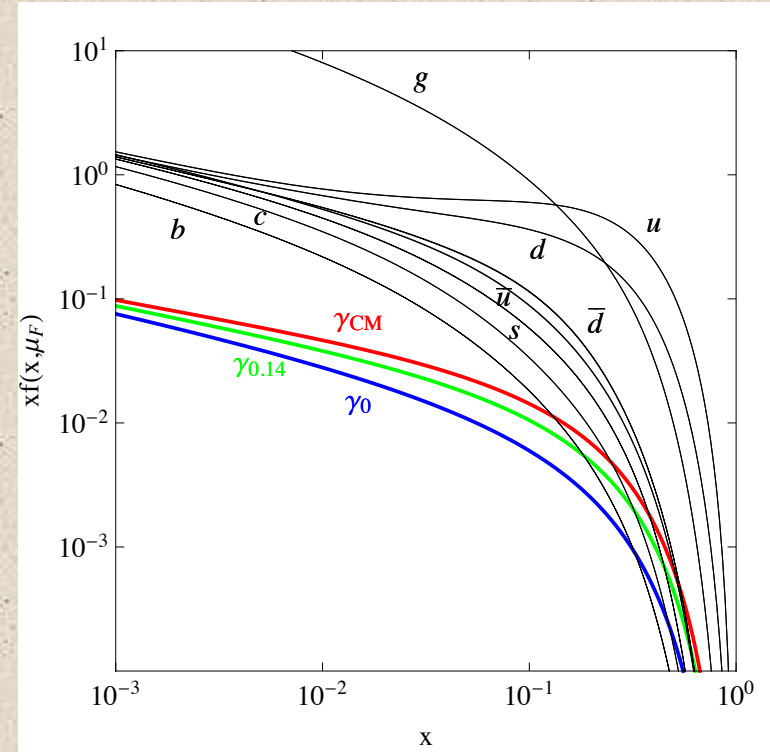
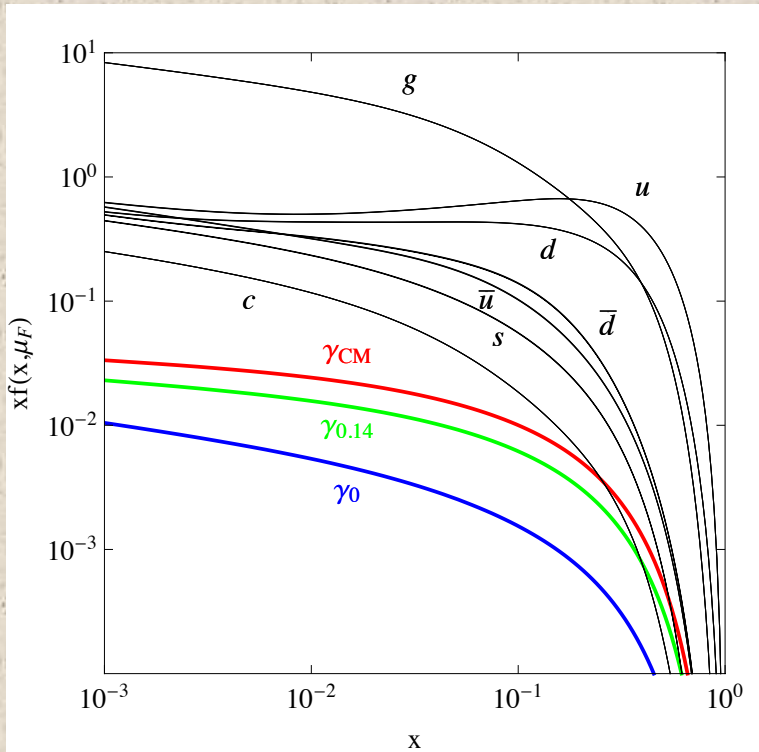
Sharp Isolation

- Different χ^2 curves for choice of isolation and scale μ_F
- 90% C.L. for $N_{pt} = 8$ corresponds to $\chi^2 = 13.36$
- Obtain $p_0^\gamma \leq 0.14\%$ at 90 % C.L. independent of isolation prescription

(More generally, constrains $\gamma(x)$ for $10^{-3} < x < 2 \times 10^{-2}$.)

- “Current Mass” ansatz has $\chi^2 > 46$ for any choice of isolation and scale

Photon PDFs (in proton)



γ momentum fraction:

$p^{\gamma}(Q)$	$\gamma(x, Q_0) = 0$	$\gamma(x, Q_0) = 0.14\%$
$Q = 3.2 \text{ GeV}$	0.05%	0.19%
$Q = 85 \text{ GeV}$	0.22%	0.35%

Photon PDF can be larger than sea quarks at large x !

Initial Photon PDF still
← significant at large Q .

Conclusions

- The CTEQ-TEA group has been very busy.
- CT14 PDFs are first CT PDFs to include LHC data.
- CT14QED PDFs are first CT PDFs to include QED evolution, necessary for consistent EW corrections
- Data from current LHC run will further constrain PDFs
- Necessary for precision SM and BSM predictions at high energy colliders

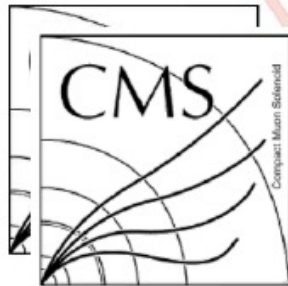
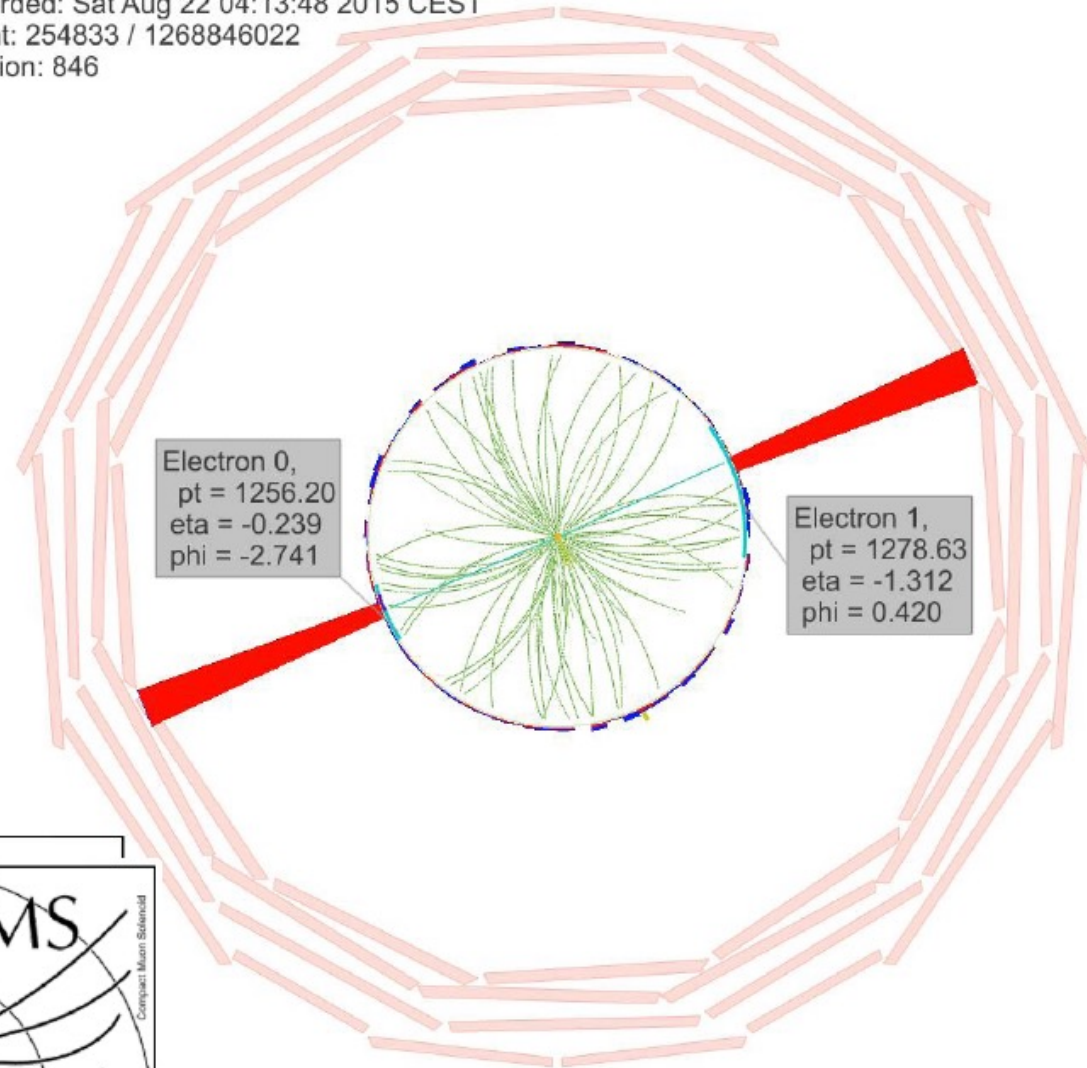


CTEQ

CMS-DP-2015-039 ; CERN-CMS-
DP-2015-039

*Event Display of a Candidate
Electron-Positron Pair with an
Invariant Mass of 2.9 TeV*

CMS Experiment at LHC, CERN
Data recorded: Sat Aug 22 04:13:48 2015 CEST
Run/Event: 254833 / 1268846022
Lumi section: 846



SM rate is small

SM Background Expectations

mass range	SM Bkg Expectation
>1 TeV	0.21
> 2 TeV	0.007
> 2.5 TeV	0.002

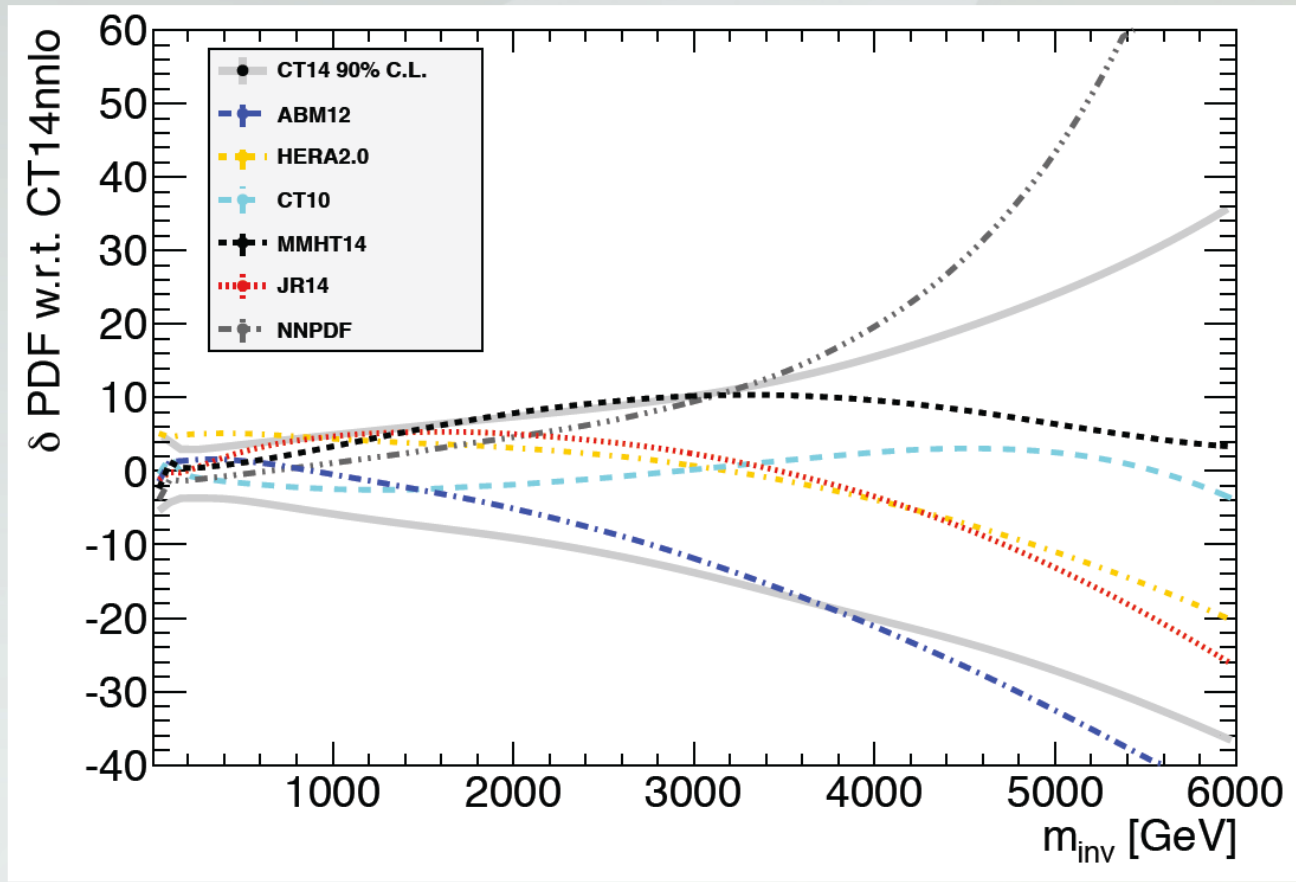
electrons are required to satisfy:
 $E_T > 35$ GeV
 $|\eta| < 1.4442$ or $1.566 < |\eta| < 2.5$
pass high energy ele selection

in addition one electron must have
 $|\eta| < 1.4442$

- the values of this table have been obtained from the mass spectrum distribution in CERN-CMS-PD-2015-037 and scaled to the luminosity of 65pb^{-1} , which is the luminosity of full 50ns dataset

SM cross section is $7.7\text{E-}3$ fb for $2.8 < M_{\{ee\}} < 3.0$ TeV.

NC DY - CT14nnlo PDF Variation, and Choice.



CT14-PDF uncertainty is about +10% -14% around 2.9 TeV, at the 68% CL.

Daniel Hayden

Backup Slides

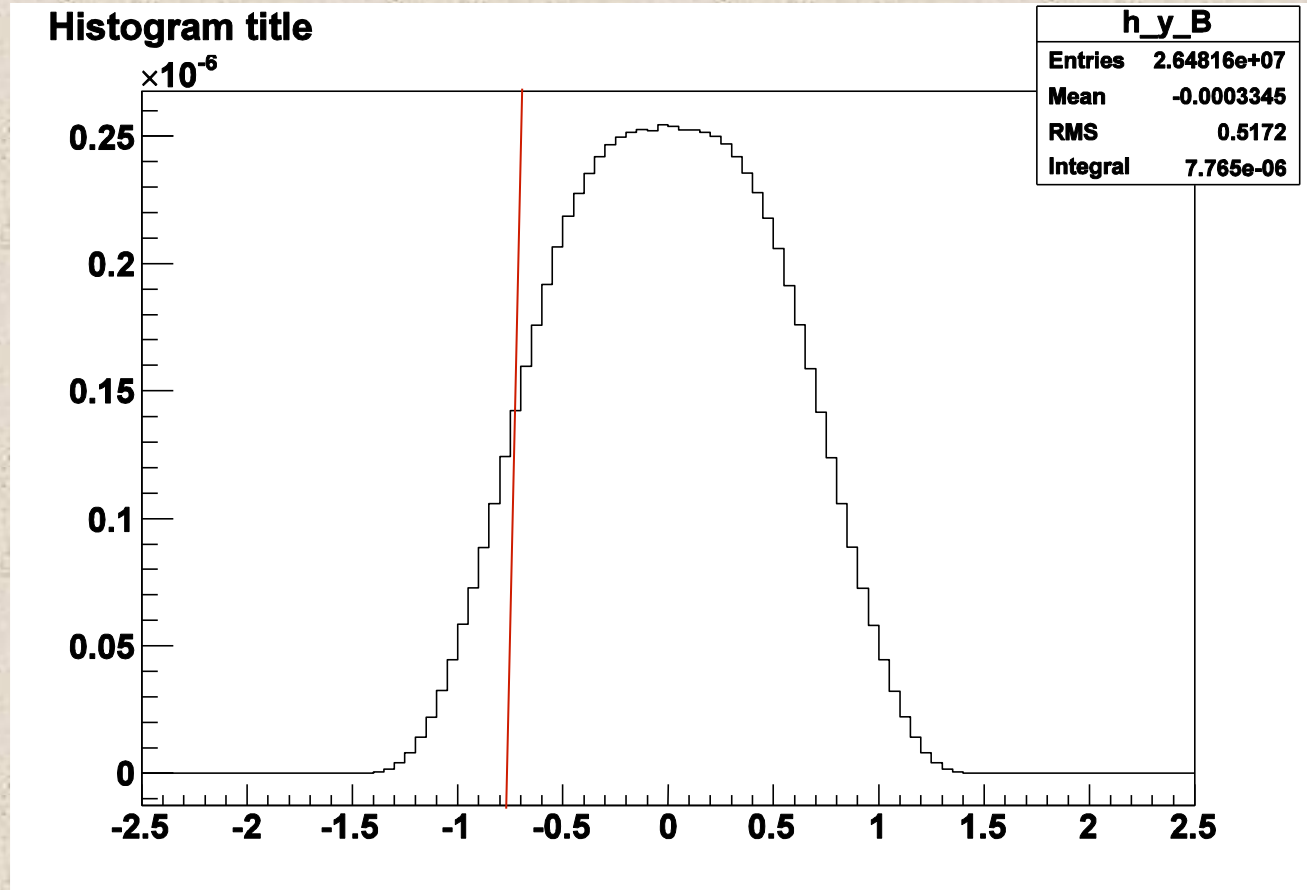
CMS @ 13 TeV LHC with 65 1/pb

Event Kinematic Details

	electron 0	electron 1
E_T	1260 GeV	1280 GeV
η	-0.24	-1.31
ϕ	-2.74 rad	0.42 rad
charge	-1	+1
mass	2.91 TeV	
$\cos \theta_{CS}^*$	-0.49	
γ	-0.78	

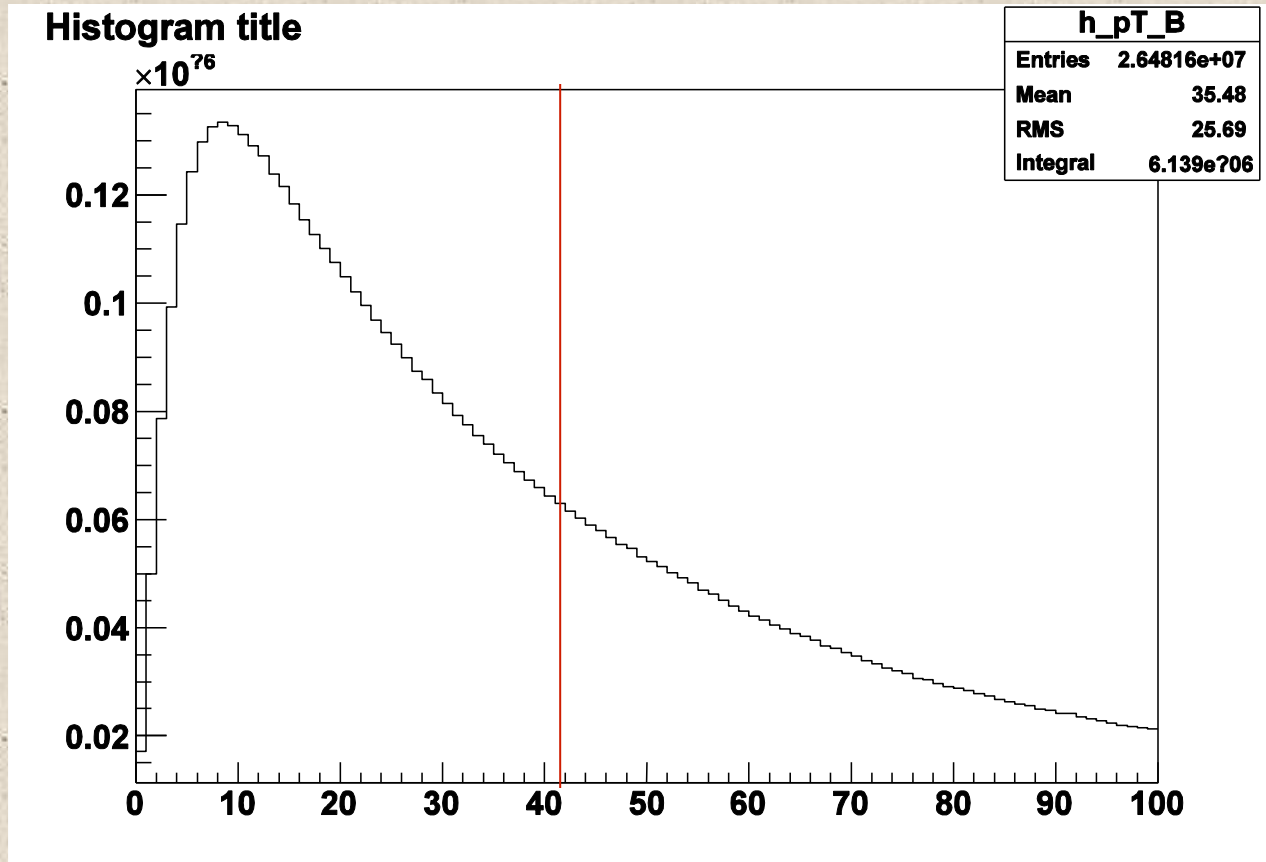
p_T of this Drell-Yan pair is 41.6 GeV, and its $p_Z < 0$

Rapidity distribution of a 2.9 TeV Drell-Yan pair



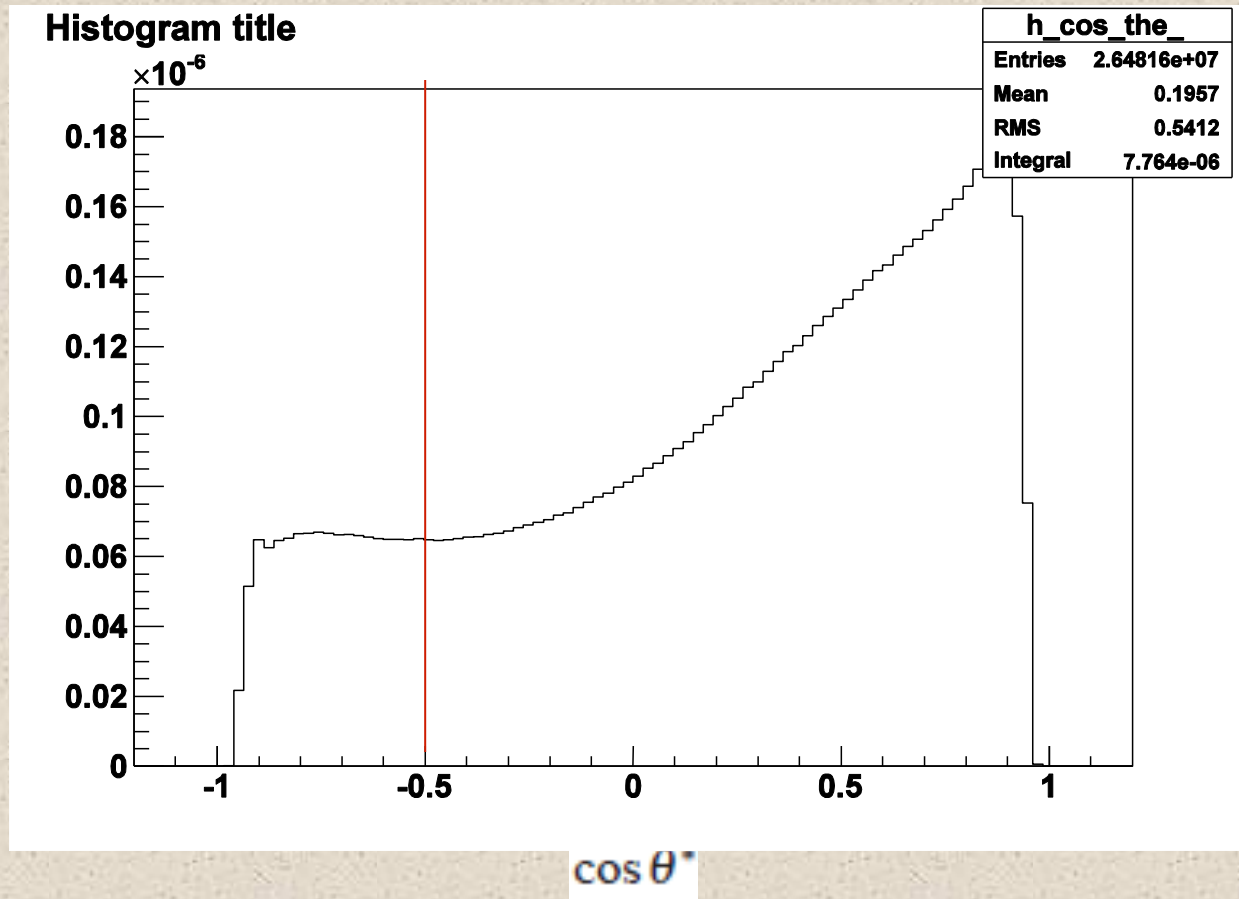
$$y = -0.78$$

pT distribution of a 2.9 TeV Drell-Yan pair



pT = 41.6 GeV

$\cos \theta^*$ distribution for a 2.9 ± 0.1 TeV Drell-Yan pair



$$\cos(\theta^*) = -0.49$$

and $P_Z < 0$

“Modified” Collins-Soper angle

The angle θ^* is then taken as the angle between this z-axis and the outgoing negatively charged lepton, using the formula

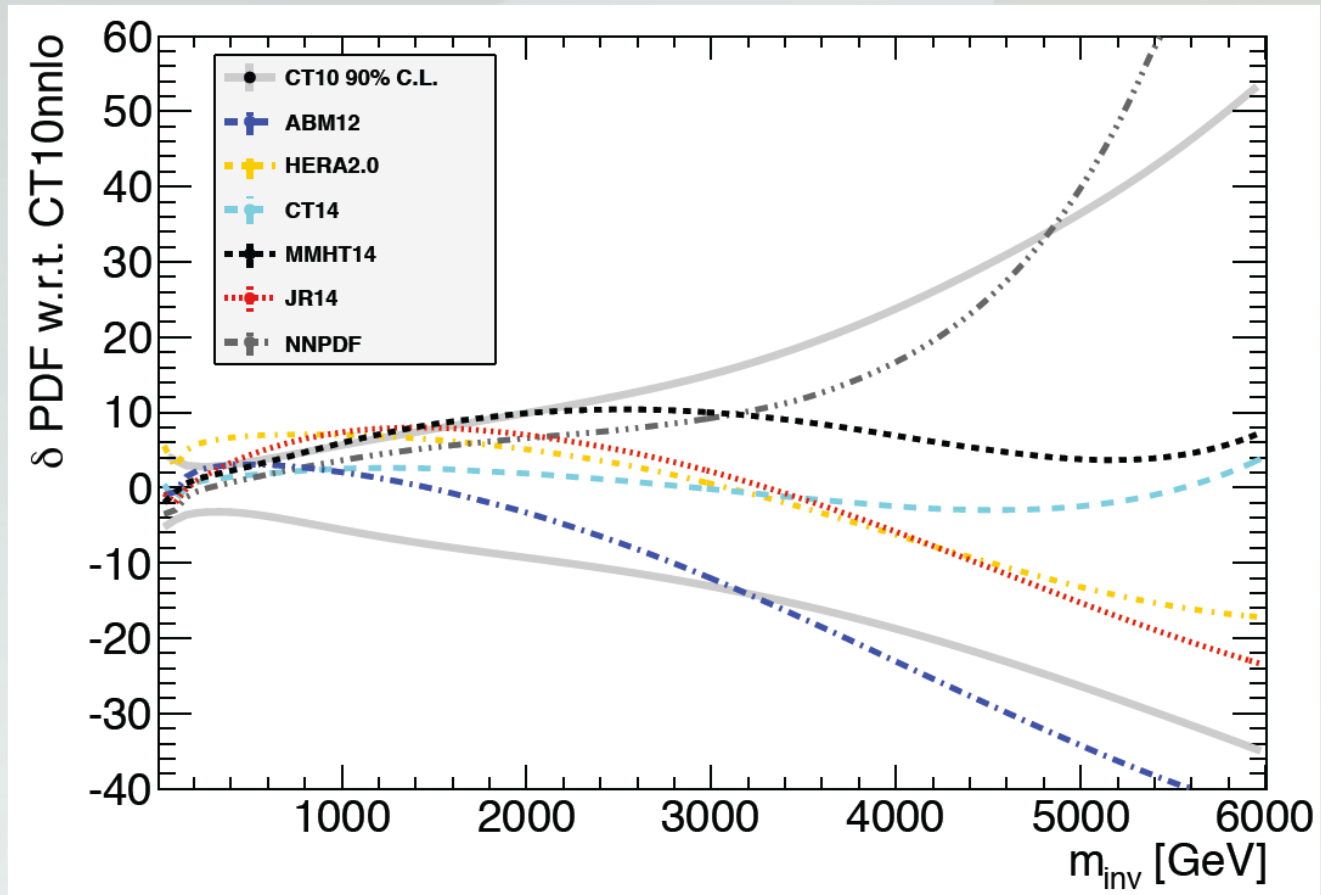
$$\cos \theta^* = \frac{p_z(\ell^+\ell^-)}{|p_z(\ell^+\ell^-)|} \frac{2(p_1^+ p_2^- - p_1^- p_2^+)}{m(\ell^+\ell^-) \sqrt{m(\ell^+\ell^-)^2 + p_T(\ell^+\ell^-)^2}},$$

where p_n^\pm denotes $\frac{1}{\sqrt{2}}(E \pm p_z)$ and $n = 1$ or 2 corresponds to the negatively charged or positively charged leptons, respectively. From this angle, a forward-backward asymmetry, which is sensitive to the chiral structure of the interaction, is defined as follows:

$$A_{\text{FB}} = \frac{N_{\text{F}} - N_{\text{B}}}{N_{\text{F}} + N_{\text{B}}},$$

where N_{F} (N_{B}) is the number of events with $\cos \theta^*$ greater (smaller) than zero.

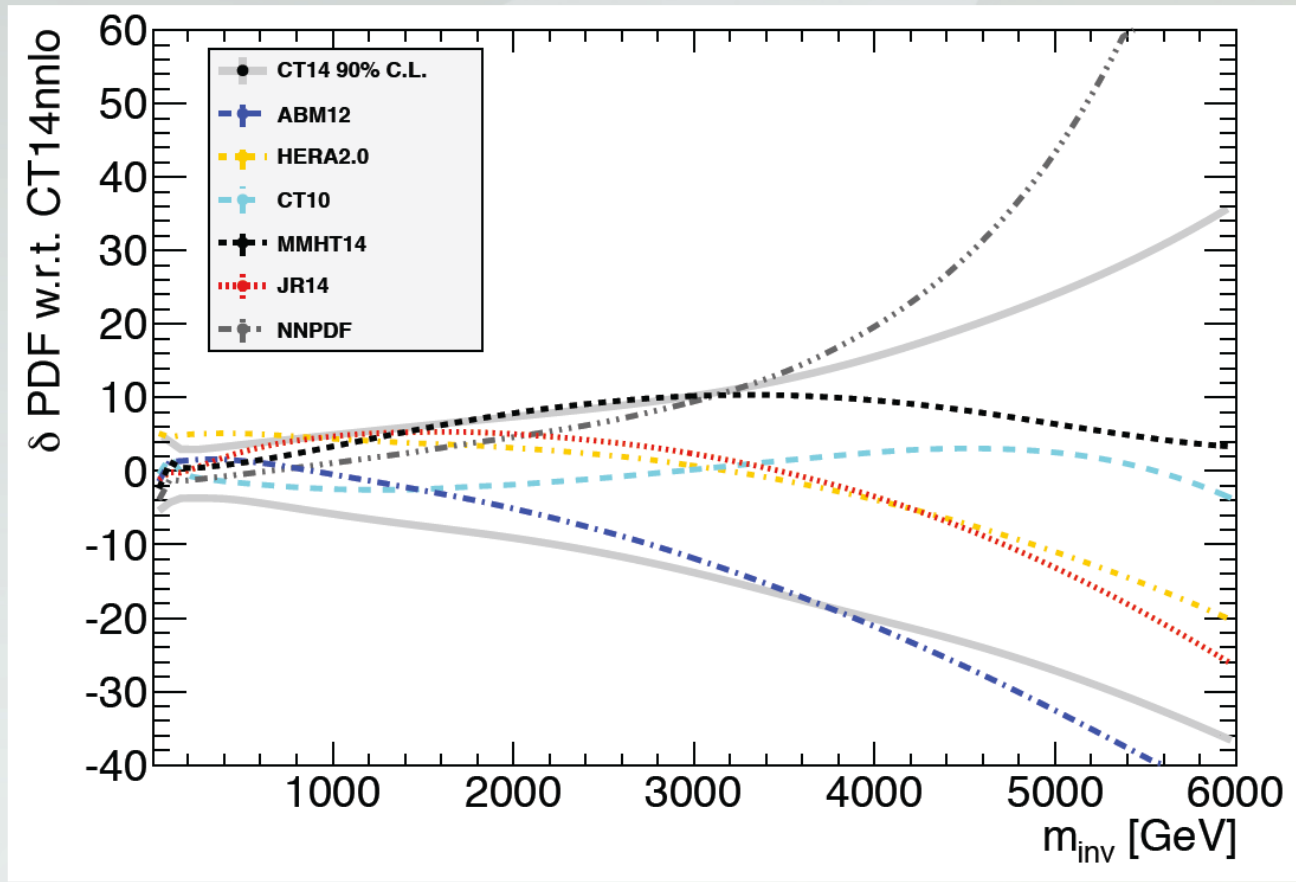
NC DY - CT10nnlo PDF Variation, and Choice.



CT10 PDF uncertainty is about $\pm 14\%$ around 2.9 TeV, at the 68% CL.

Daniel Hayden

NC DY - CT14nnlo PDF Variation, and Choice.



CT14-PDF uncertainty is about +10% -14% around 2.9 TeV, at the 68% CL.

Daniel Hayden

Constraining Photon PDFs

1) Global fitting

- Isospin violation, momentum sum rule lead to constraints in fit
- We find p_0^γ can be as large as $\sim 5\%$ at 90%CL, much more than **CM** choice

2) Direct photon PDF probe

- DIS with observed photon, $ep \rightarrow e\gamma + X$
- Photon-initiated subprocess contributes at LO, and no larger background with which to compete
- But must include quark-initiated contributions consistently
- Treat as NLO in α , but discard small corrections, suppressed by $\alpha \gamma(x)$.

$$ep \rightarrow e\gamma + X$$

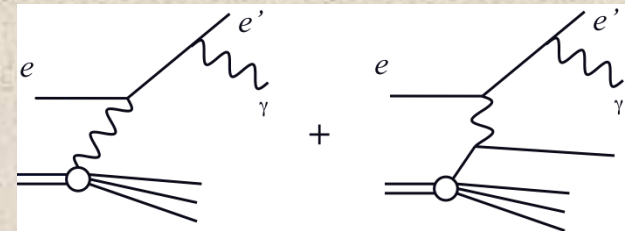
Subprocess contributions:

LL Emission off Lepton line

Both quark-initiated and photon-initiated contributions are $\sim \alpha^3$ if $\gamma(x) \sim \alpha$

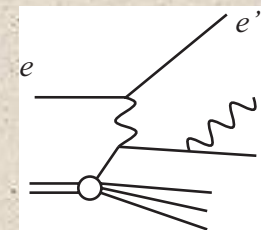
Collinear divergence cancels (in $d=4-2\varepsilon$) by treating as

$$\text{NLO in } \alpha \text{ with } \gamma^{\text{bare}}(x) = \gamma(x) + \frac{(4\pi)^\varepsilon}{\varepsilon} \Gamma(1+\varepsilon) \frac{\alpha}{2\pi} (P_{\gamma q} \circ q)(x) \quad (\overline{\text{MS}})$$



QQ Emission off Quark line

Has final-state quark-photon collinear singularity



QL Interference term

Negligible < about 1% (but still included)

Previous calculations:

quark-initiated only – (GGP) Gehrmann-De Ridder, Gehrmann, Poulson, PRL 96, 132002 (2006)

photon initiated only – (MRST), Martin, Roberts, Stirling, Thorne, Eur. Phys. J. C 39, 155 (2005)

Zeus Experimental Cuts

Photon Cuts

$$4 \text{ GeV} < E_T^\gamma < 15 \text{ GeV}$$

$$-0.7 < \eta^\gamma < 0.9$$

Lepton Cuts

$$E_{\ell'} > 10 \text{ GeV}$$

$$139.8^\circ < \theta_{\ell'} < 171.8^\circ$$

$$10 \text{ GeV}^2 < Q^2 < 350 \text{ GeV}^2$$

Photon Isolation Cut

Photon must contain 90% of energy in jet to which it belongs.

Also require $N \geq 1$ forward jet

Two theoretical approximations to photon isolation implemented:

1) Smooth isolation (Frixione): $E_{q'} < \frac{1}{9} E_\gamma \left(\frac{1 - \cos r}{1 - \cos R} \right)$ for $r = \sqrt{\Delta\eta_{q'\gamma}^2 + \Delta\varphi_{q'\gamma}^2} < R = 1$

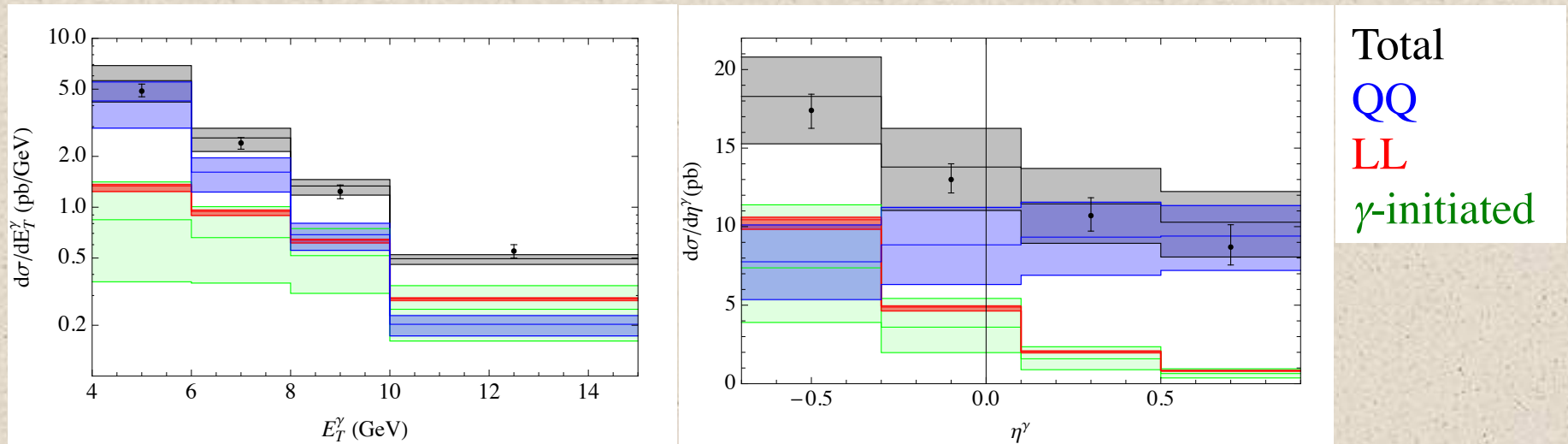
- Removes fragmentation contribution

2) Sharp isolation: $E_{q'} < \frac{1}{9} E_\gamma$ for $r < R = 1$

- Requires fragmentation contribution
(Use Aleph LO parametrization)

Theoretical Uncertainties

1) Factorization Scale

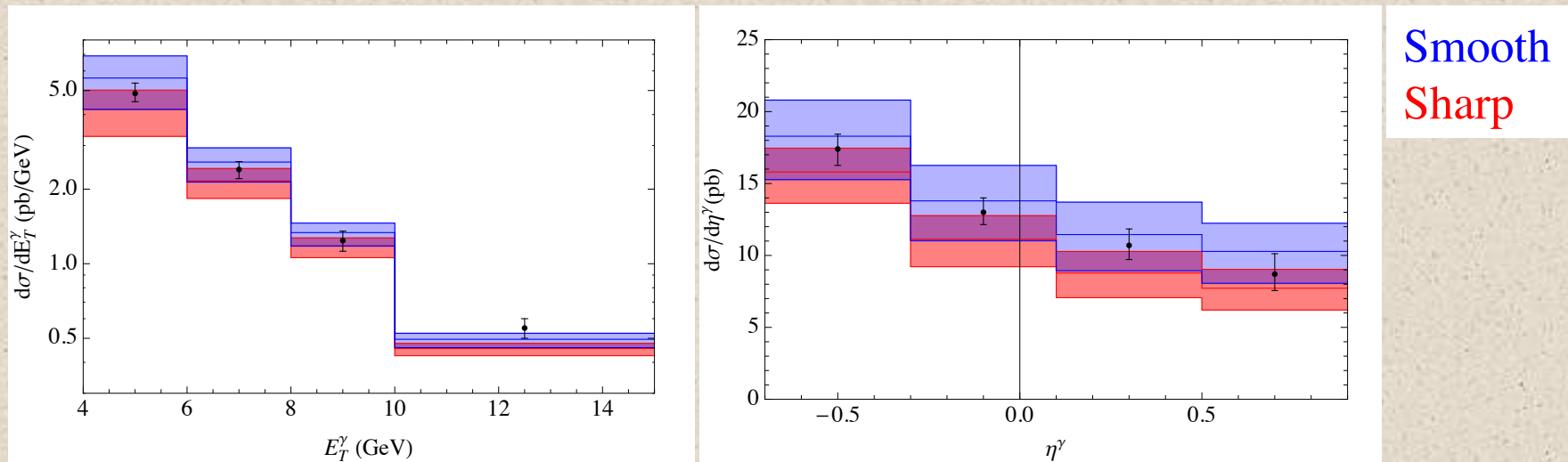


($p_0^\gamma = 0$, Smooth Isolation, $0.5E_T^\gamma < \mu_F < 2E_T^\gamma$)

- Scale dependence of **LL** contribution reduced drastically compared to photon-initiated alone
- **QQ** and **LL** have different-shaped distributions. **LL** dominates at large E_T^γ and small η^γ . Can be used to extract photon PDF
- Scale dependence of **QQ** and total is still large (LO in α_S)

Theoretical Uncertainties

2) Isolation Prescription

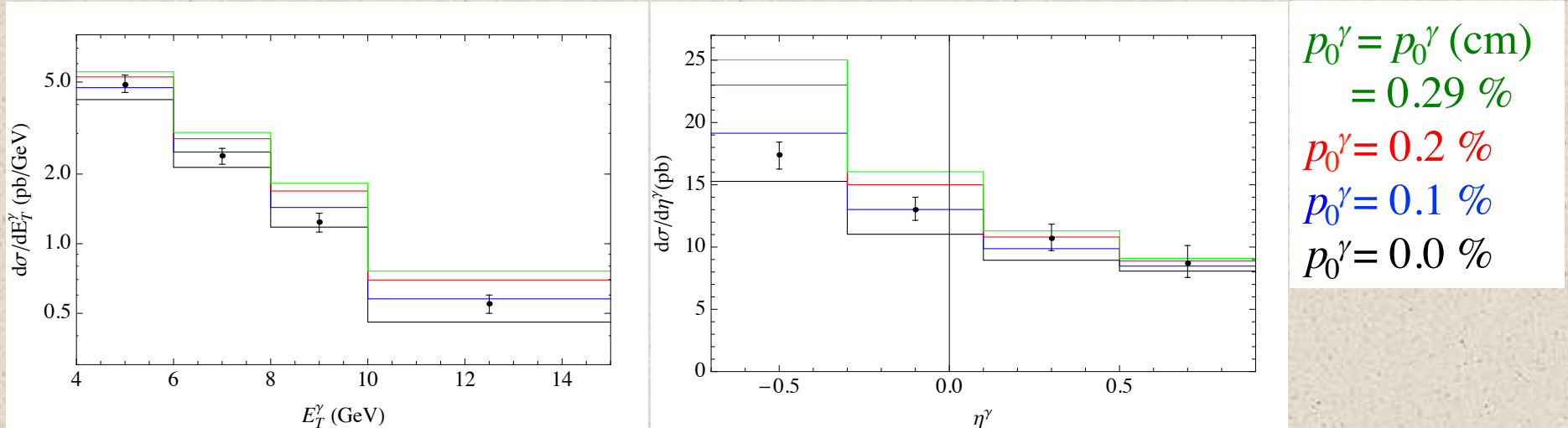


$$(p_0^\gamma = 0, 0.5E_{T\gamma} < \mu_F < 2E_{T\gamma})$$

- Difference between two isolation prescriptions is about same size as scale uncertainty
- Smooth prescription gives larger predictions. In principle, should give smaller.
- Uncertainty in fragmentation function, and higher order effects in both prescriptions are major sources of difference.
- Use both prescriptions as measure of uncertainty in prediction.

Distributions

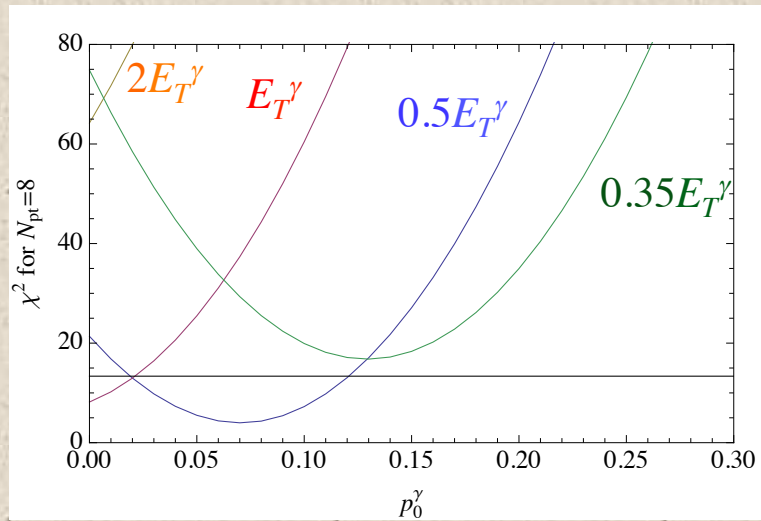
1) Photon Variables E_T^γ and η^γ



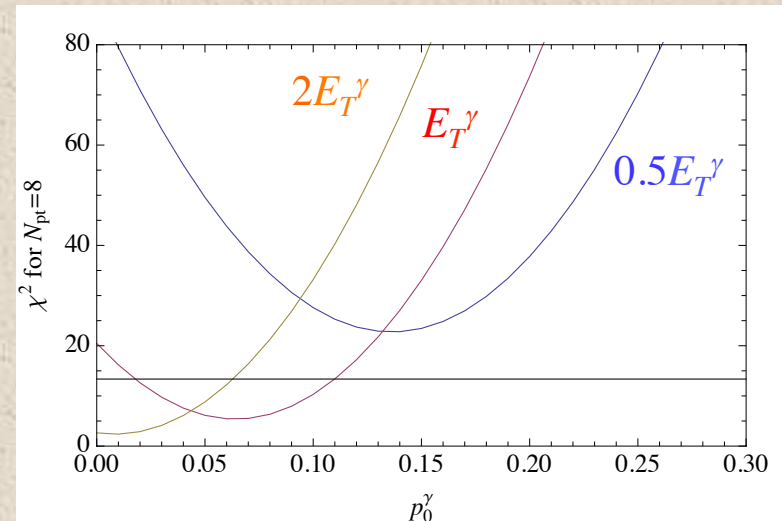
(Smooth Isolation, $\mu_F = 0.5E_T^\gamma$)

- Best fit for p_0^γ is correlated with choice of isolation and factorization scale μ_F .
- Can obtain excellent fit to shape of distributions for reasonable scale choices.
- “Current Mass” ansatz cannot fit shape (prediction too large at large E_T^γ and small η^γ where **LL** dominates), regardless of scale choice.

Limits on Photon PDF



Smooth Isolation



Sharp Isolation

- Different χ^2 curves for choice of isolation and scale μ_F
- 90% C.L. for $N_{pt} = 8$ corresponds to $\chi^2 = 13.36$
- Obtain $p_0^\gamma \leq 0.14\%$ at 90 % C.L. independent of isolation prescription

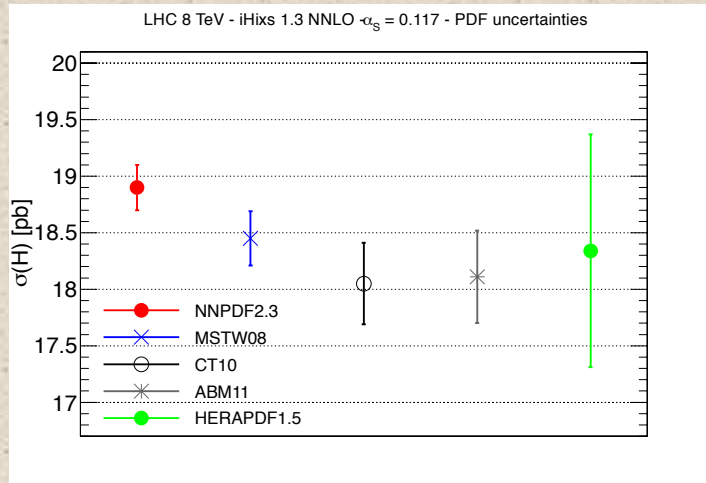
(More generally, constrains $\gamma(x)$ for $10^{-3} < x < 2 \times 10^{-2}$.)

- “Current Mass” ansatz has $\chi^2 > 45$ for any choice of isolation and scale

Conclusions

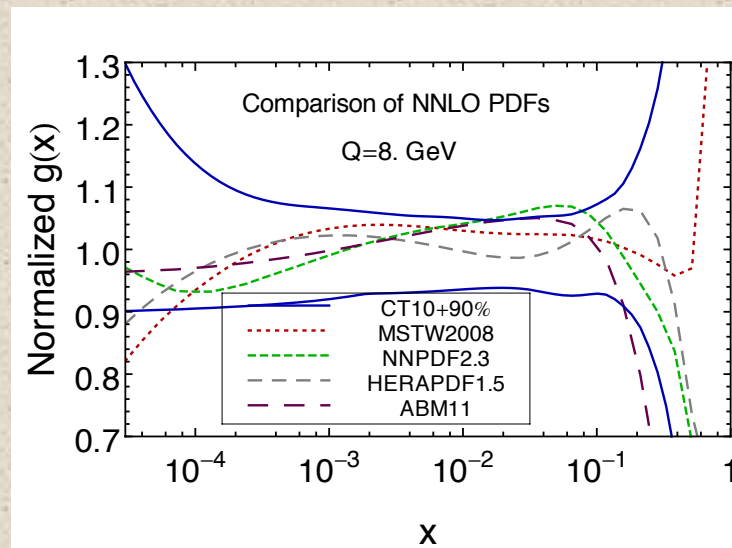
- CT1X update in progress
 - New LHC data, New parametrizations, ...
- CT10 IC sets available
- CT10 H extreme sets for Higgs studies available
 - LM analysis confirms standard Hessian for this process
- Photon PDF
 - Strong constraint from $ep \rightarrow e\gamma + X$
 - $p_0^\gamma \leq 0.14\%$ at 90 % C.L. for radiative photon ansatz.
 - Consistent with NNPDF Drell-Yan analysis:
Photon PDF smaller than predicted by current mass ansatz

PDF Benchmarking and MetaPDFs



Benchmarking-
Ongoing study to compare and understand differences in PDF predictions at LHC

Ball et al, JHEP 1304 (2013) 125



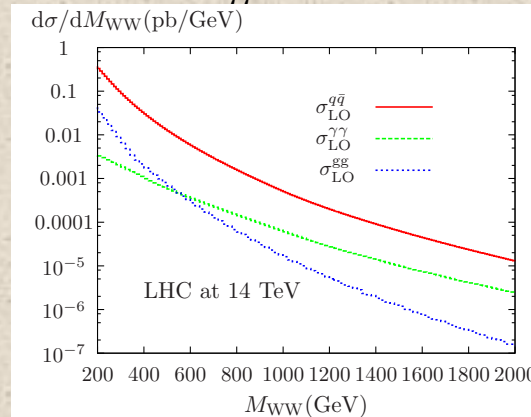
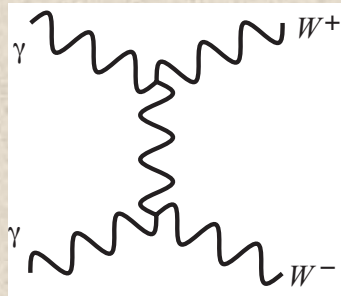
MetaPDFs-
Combine different PDF groups in a Meta-PDF set, to compare systematic uncertainties

Gao and Nadolsky, arXiv:1401.0013[hep-ph]

Motivation

- 1) Sensitivity to NNLO QCD is at few % level.
 - QED and Electroweak corrections are now significant.
 - E.g, QED corrections to $pp \rightarrow W + X$ require order α effects in parton evolution
- 2) Photon induced processes can be kinematically enhanced.

$$\gamma\gamma \rightarrow W^+W^- \text{ asymptotically } \hat{\sigma}_{\gamma\gamma} \approx 8\pi\alpha^2 / M_W^2$$



Bierweiler et al.,
JHEP 1211 (2012) 093

- 3) Last considered in 2004 (MRST) Martin et al., EPJC 39 (2005) 155.
 - Time for more detailed study.

This talk is an update of CTEQ-TEA activities on this topic.

Inclusion of Photon PDFs

LO QED + (NLO or NNLO) QCD evolution:

$$\frac{dq}{dt} = \frac{\alpha_s}{2\pi} (P_{qq} \circ q + P_{qg} \circ g) + \frac{\alpha}{2\pi} (e_q^2 \tilde{P}_{qq} \circ q + e_q^2 \tilde{P}_{q\gamma} \circ \gamma)$$

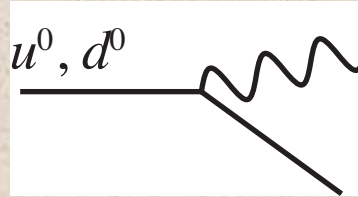
$$\frac{dg}{dt} = \frac{\alpha_s}{2\pi} (P_{gg} \circ g + P_{gq} \circ \sum (q + \bar{q}))$$

$$t = \ln Q^2$$

$$\frac{d\gamma}{dt} = \frac{\alpha}{2\pi} (\tilde{P}_{\gamma\gamma} \circ \gamma + \tilde{P}_{\gamma q} \circ \sum e_q^2 (q + \bar{q}))$$

“Radiative ansatz” for initial Photon PDFs (generalization of MRST choice)

$$\gamma^p = \frac{\alpha}{2\pi} (A_u e_u^2 \tilde{P}_{\gamma q} \circ u^0 + A_d e_d^2 \tilde{P}_{\gamma q} \circ d^0)$$



$$\gamma^n = \frac{\alpha}{2\pi} (A_u e_u^2 \tilde{P}_{\gamma q} \circ d^0 + A_d e_d^2 \tilde{P}_{\gamma q} \circ u^0)$$

where u^0 and d^0 are “primordial” valence-type distributions of the proton.

Assumed approximate isospin symmetry for neutron.

Here, we take A_u and A_d as unknown fit parameters.

MRST choice: $A_q = \ln(Q_0^2/m_q^2)$ “Radiation from Current Mass” - CM 49

Inclusion of Photon PDFs (2)

Isospin violation occurs radiatively in u and d. To this order in α :

$$u^n = d^p + \frac{\alpha}{2\pi} (A_u e_u^2 - A_d e_d^2) \tilde{P}_{qq} \circ d^0, \quad d^n = u^p + \frac{\alpha}{2\pi} (A_d e_d^2 - A_u e_u^2) \tilde{P}_{qq} \circ u^0$$



Isospin violation in initial sea and gluon assumed negligible. ($\bar{q}^n = \bar{q}^p, g^n = g^p$)

With this ansatz, number and momentum sum rules automatically satisfied for neutron, for any choice of u^0 and d^0 .

$$i.e., \sum p^{i/P} = 1 \Rightarrow \sum p^{i/N} = 1, \text{ where } p^{i/h} = \int_0^1 x f_{i/h}(x) dx$$

Here, assume $u^0 = u^p \equiv u^p(x, Q_0), \quad d^0 = d^p \equiv d^p(x, Q_0)$

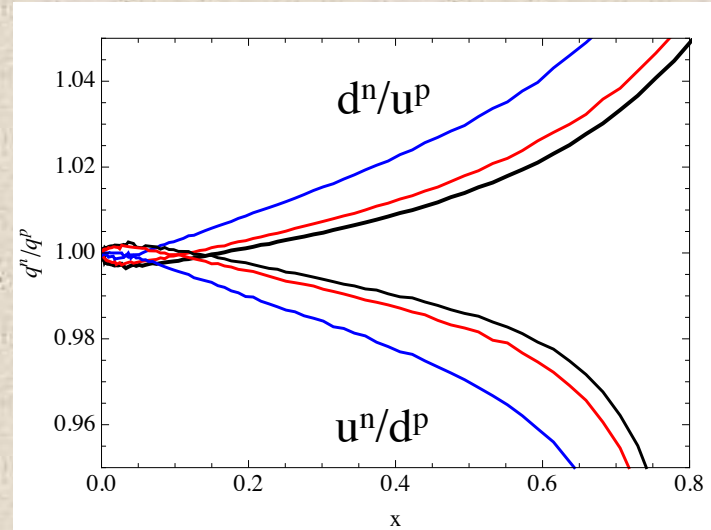
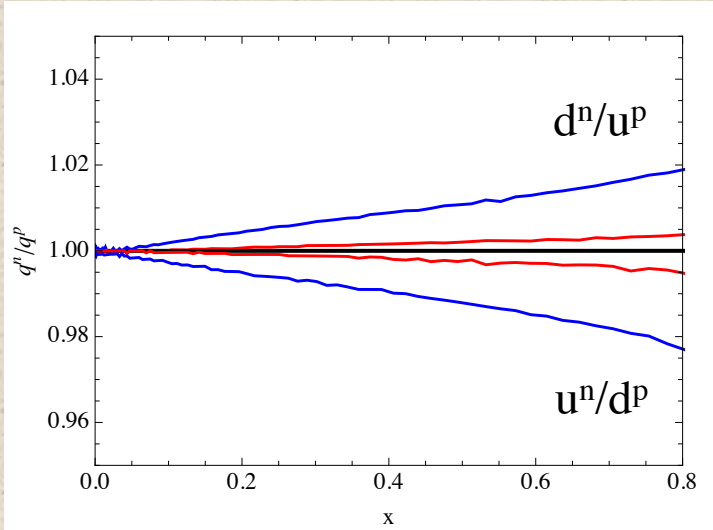
Also, let $A_u = A_0(1 + \delta), \quad A_d = A_0(1 - \delta)$

Expect δ to be small.

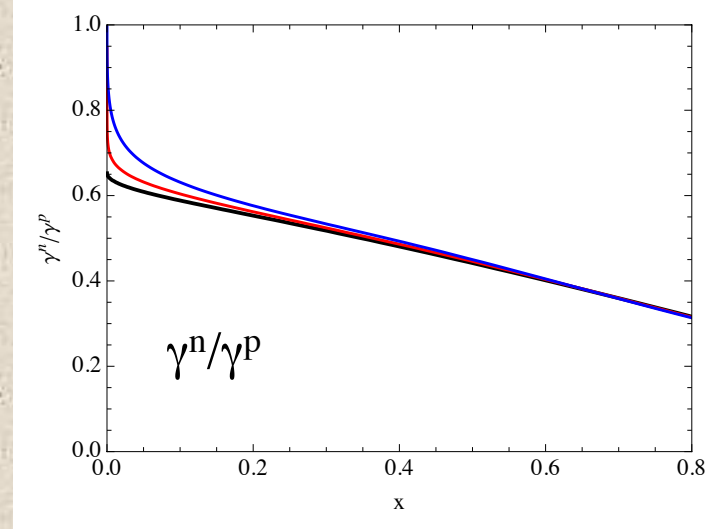
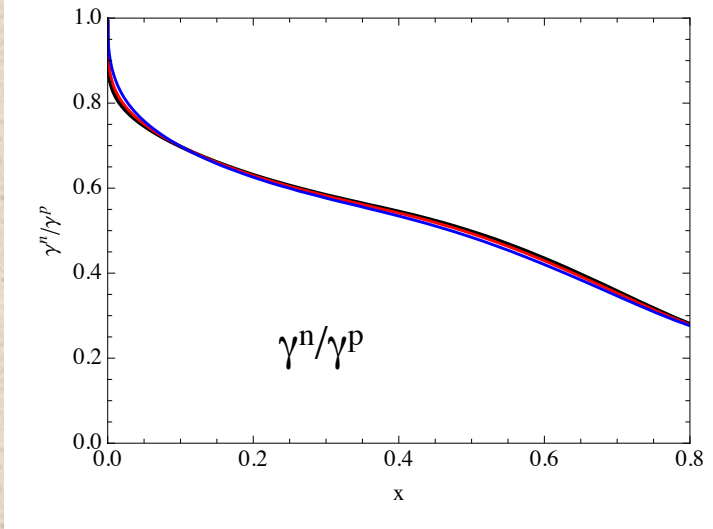
Now everything effectively specified by one unknown parameter:

$$A_0 \Leftrightarrow p_0^\gamma \equiv p^{\gamma/P}(Q_0) \quad (\text{Initial Photon momentum fraction})$$

Isospin violation



$Q=Q_0=1.3 \text{ GeV}$
 $Q=3.2 \text{ GeV}$
 $Q=85 \text{ GeV}$



$$\gamma(x, Q_0^2) = 0$$

$$\gamma(x, Q_0^2)_{\text{CM}}$$

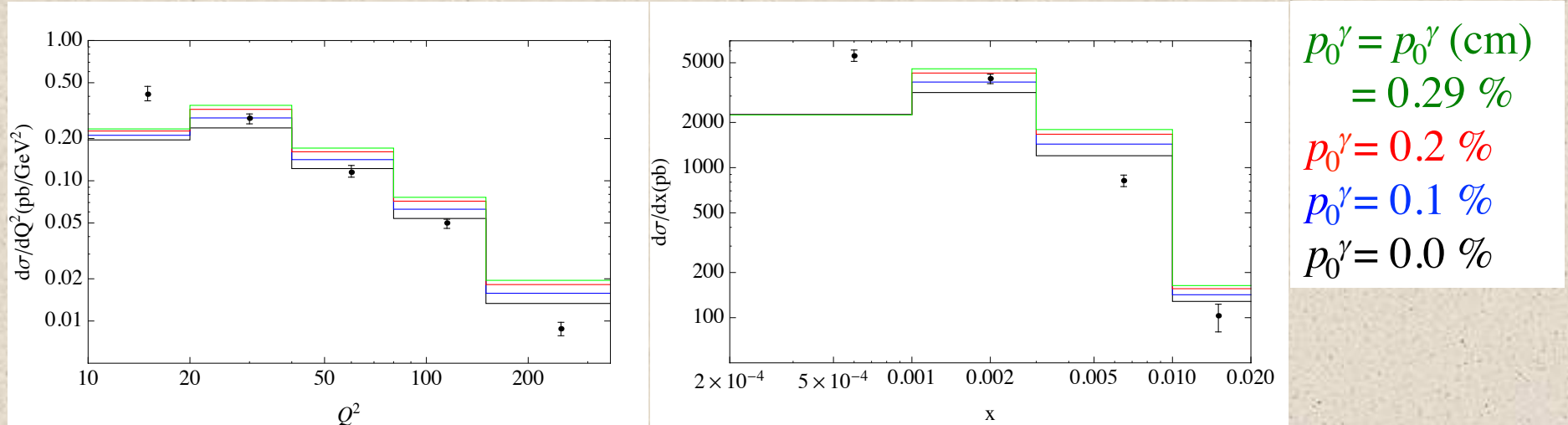
Constraints on Photon PDFs

- 1) Global fitting
 - a. Isospin violation effects
 - come from scattering off nuclei
 - perturbativity cuts on W^2 generally require $x < .2-.4$
 - constraints likely to be small (MRST)
 - b. Momentum sum rule
 - momentum carried by photon leaves less for other partons
 - constrains momentum fraction of photon (upper bound)
 - c. Otherwise, $O(\alpha)$ corrections to hadronic processes are small
 - d. Global fit finds p_0^γ can be as large as $\sim 5\%$, much more than **CM** choice

- 2) Direct photon PDF probe
 - DIS with observed photon, $ep \rightarrow e\gamma + X$
 - Photon-initiated subprocess contributes at LO !

Distributions

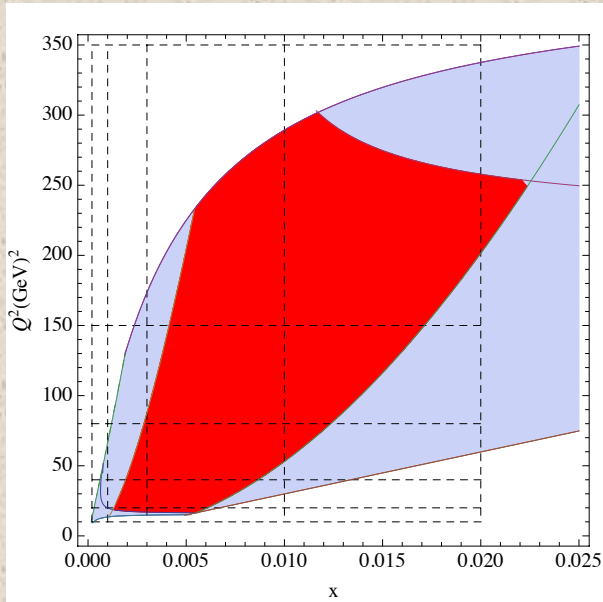
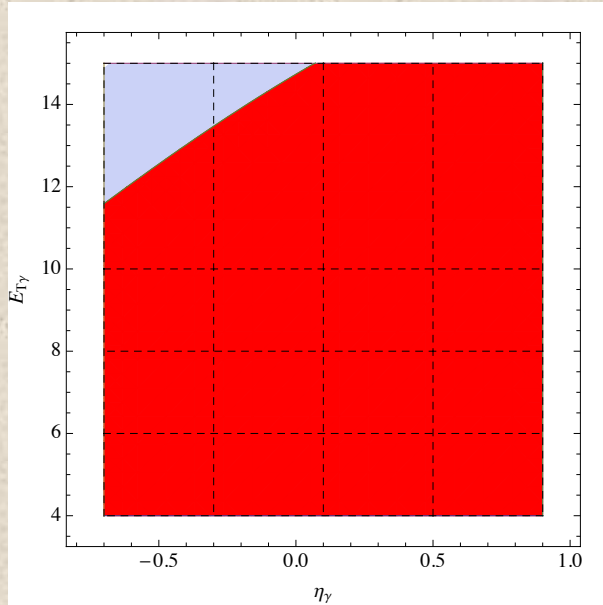
2) Lepton Variables Q^2 and x



(Smooth Isolation, $\mu_F = 0.5E_T^\gamma$)

- Cannot fit shape for any choice of isolation, scale, or p_0^γ .
- Q^2 and x distributions more sensitive to higher order corrections.
 (Small Q^2 and x , in particular will receive contributions from more radiation.)
- Additional cuts on E_T^γ and η^γ make Q^2 and x distributions less inclusive.

Kinematic Phase Space



Photon Cuts

$$4 \text{ GeV} < E_T^\gamma < 15 \text{ GeV}$$

$$-0.7 < \eta^\gamma < 0.9$$

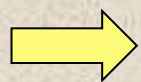
Lepton Cuts

$$E_{\ell'} > 10 \text{ GeV}$$

$$139.8^\circ < \theta_{\ell'} < 171.8^\circ$$

$$10 \text{ GeV}^2 < Q^2 < 350 \text{ GeV}^2$$

- Dashed lines show kinematic bins
- Red region allowed for “photon + lepton + 0 additional partons”
(LO photon-initiated kinematics)
- Red plus Blue region allowed for “photon + lepton + anything”
- Q^2 and x distributions more affected by additional photon cuts.
- Smallest x bin requires ≥ 1 extra parton to satisfy cuts.



Use only E_T^γ and η^γ distributions to constrain photon PDF